

PONTIFÍCIA UNIVERSIDADE CATÓLICA
DO RIO DE JANEIRO



Behbood Abedi

**Startup Flow of Gelled Crude Oils: an
Experimental Study**

Dissertação de Mestrado

Dissertation presented to the Programa de Pós-Graduação em Engenharia Mecânica of the Departamento de Engenharia Mecânica, PUC-Rio, as partial fulfillment of the requirements for the degree of Mestre em Engenharia Mecânica.

Advisor: Prof. Paulo Roberto de Souza Mendes

Rio de Janeiro
February 2016



Behbood Abedi

**Startup Flow of Gelled Crude Oils: an
Experimental Study**

Dissertation presented to the Programa de Pós-Graduação em Engenharia Mecânica of the Departamento de Engenharia Mecânica do Centro Técnico Científico da PUC-Rio, as partial fulfillment of the requirements for the degree of Mestre em Engenharia Mecânica.

Prof. Paulo Roberto de Souza Mendes

Advisor

Departamento de Engenharia Mecânica - PUC-Rio

Prof. Mônica Feijó Naccache

Departamento de Engenharia Mecânica - PUC-Rio

Prof. Roney Leon Thompson

UFF

Prof. Márcio da Silveira Carvalho

Coordinator of the Centro Técnico Científico da PUC-Rio

Rio de Janeiro, February 26th, 2016

All rights reserved.

Behbood Abedi

Graduated in Petroleum Engineering from the Petroleum University of Technology (Iran-2008), and holds a Master's degree in Chemical Engineering from the same university (2011). He has some experience in Core Analysis and Enhanced Oil Recovery laboratories.

Bibliographic data

Abedi, Behbood

Startup Flow of Gelled Crude Oils: an Experimental Study / Behbood Abedi; adviser: Paulo Roberto de Souza Mendes. – 2016.

62 f. : il. color. ; 30 cm

Dissertação (mestrado) - Pontifícia Universidade Católica do Rio de Janeiro, Departamento de Engenharia Mecânica, 2016.

Inclui bibliografia

1. Engenharia Mecânica – Teses. 2. Fluidos com Tensão de Cedência. 3. Óleo Cru Gelificado. 4. Reinício de Escoamento. 5. Deslizamento na Parede. I. de Souza Mendes, Paulo Roberto. II. Pontifícia Universidade Católica do Rio de Janeiro. Departamento de Engenharia Mecânica. III. Título.

CDD: 621

Acknowledgments

At the end of my thesis I would like to thank all those people who made this thesis possible and an unforgettable experience for me. First of all, I would like to express my deepest sense of Gratitude to my supervisor Prof. Paulo Roberto de Souza Mendes, who offered his continuous advice and encouragement throughout the course of this thesis. I am thankful to Fabio Martins and my colleagues at Group of Reology. This work would not have been possible without support from FAPERJ.

Abstract

Abedi, Behbood; de Souza Mendes, Paulo Roberto (advisor).
Startup Flow of Gelled Crude Oils: an Experimental Study.
Rio de Janeiro, 2016. 62p. MSc. Dissertation — Departamento de
Engenharia Mecânica, Pontifícia Universidade Católica do Rio de
Janeiro.

Besides an increasing economic importance of producing wax-containing crude oil from ultra deep water resources, concerns about wax deposition and gelation play a significant role in this area. Gelled waxy crude oils often exhibit rheological behavior analogous to yield stress fluids. There is a critical or range of stresses, below which no flow occurs, but above which the viscosity of a gelled system decreases drastically. Thus, in order to restart flow of a gelled crude, a pressure larger than the typical operating pressure should be applied to exceed the yield stress of the fluid at wall, this required minimum pressure should be determined. In this study to explore the minimum pressure notion, yield stress fluids were investigated comprehensively. The investigation was initiated with simpler yield stress fluid and then advanced with thixotropic one using rheometer and designed experimental setup for fluid flow into tube. In both cases no-slip condition was achieved, the behavior of yield stress fluids was screened in detail, the outcomes of fluid transport in tube and rheometric tests were combined and cross checked. Finally with putting all together, the required minimum pressure or in other words, the critical shear stress needed to startup the flow of yield stress fluids was discovered.

Keywords

Yield Stress Fluid; Gelled Crude Oil; Startup Flow; Wall Slip;

Resumo

Abedi, Behbood; de Souza Mendes, Paulo Roberto . **Reinício de Escoamento de Óleo Cru Gelificado: Um Estudo Experimental**. Rio de Janeiro, 2016. 62p. Dissertação de Mestrado — Departamento de Engenharia Mecânica, Pontifícia Universidade Católica do Rio de Janeiro.

Além de uma crescente importância econômica da produção de petróleo contendo parafina dos recursos águas ultra-profundas, as preocupações com a deposição e gelificação de parafina desempenha uma função significativa nesta questão. Óleos parafínicos gelificados frequentemente exibem comportamento reológico análogo para fluidos com tensão de cedência. Existe uma tensão crítica, abaixo do qual nenhum fluxo ocorre, mas acima do qual a viscosidade de um sistema gelificado diminui drasticamente. Assim, para reinício de escoamento de óleo cru gelificado, uma pressão maior do que a pressão de funcionamento normal deve ser aplicada para exceder a tensão de cedência do fluido na parede, esta pressão mínima exigida deve ser determinada. Neste estudo para explorar o conceito de pressão mínima, fluidos com tensão de cedência foram investigados inteiramente. A investigação foi iniciada com o fluido de tensão de cedência simples e, em seguida, avançou com um tixotrópico usando reômetro e configuração experimental para escoamento de fluido em tubo. Em ambos, os casos a condição "não deslizamento" foi atingida, o comportamento de fluidos com tensão de cedência foi examinado em detalhe, os resultados de experimentos de reometria e transporte de fluido em tubos foram verificados. Com a colocação de todos juntos, a pressão mínima exigida ou em outra palavra a tensão crítica para partida de escoamento de fluidos com tensão de cedência foi descoberta.

Palavras-chave

Fluidos com Tensão de Cedência; Óleo Cru Gelificado; Reinício de Escoamento; Deslizamento na Parede;

Contents

1	Introduction	11
1.1	Scope of Thesis and Roadmap	11
2	Background of Study	13
2.1	Yield Stress Fluids	13
2.2	Wall Slip	15
2.3	Wall Slip and Yield Stress Fluid	16
2.4	Slip Control	17
3	Experimentation	19
3.1	Rheometry	19
3.1.1	The AR-G2 Magnetic Bearing Rheometer	19
3.1.2	Geometries	20
3.2	Fluid Transport in Tube	24
3.2.1	Experimental Setup	24
3.3	Newtonian Fluid	28
3.4	Simple or Thixotropic?	30
3.5	Simple Yield Stress Fluid	32
3.6	Thixotropic Yield Stress Fluid	37
3.6.1	Preparation Scheme	38
4	Final Discussion	49

List of Figures

3.1	Rheometer AR-G2	19
3.2	Crosshatched plate	21
3.3	Crosshatched roughness	21
3.4	Sandblasted plate	22
3.5	Sandblasted roughness	22
3.6	DIN Rotor	23
3.7	DIN Rotor and Standard Cup	23
3.8	Grooved Recessed-End Rotor	24
3.9	Grooved Recessed-End Rotor and Grooved Cup	24
3.10	Bolted plates enclosing a snaked-like tube	25
3.11	Top and side view of single plate containing semi-circle tube	25
3.12	Manometer for pressures less than 1 bar	26
3.13	Manometer for pressures larger than 1 bar	26
3.14	Experimental setup - fluid transport in tube	27
3.15	Wall roughness along tube	27
3.16	Glycerol viscosity	28
3.17	Calculated radius using Hagen-Poiseuille law	29
3.18	Commercial hair gel - thixotropy, Test 1	30
3.19	Aqueous solution of Laponite - thixotropy, Test 1	30
3.20	Commercial hair gel - thixotropy, Test 2	31
3.21	Aqueous solution of Laponite - thixotropy, Test 2	31
3.22	Rheometric tests - hair gel	32
3.23	Flow curve - hair gel	32
3.24	Creep flow test - hair gel	33
3.25	Flow curve 1 - hair gel	34
3.26	Flow curve 2 - hair gel	35
3.27	Flow curve 3 - hair gel	35
3.28	Experimental data and Herschel-Bulkley solution	36
3.29	Rheometric tests - aqueous Laponite suspension	37
3.30	$C_s - C_w$ Phase diagram of Laponite solution	38
3.31	Shear history effect	42
3.32	Structure destruction due to applied shear rates	42
3.33	Structure build-up with applying a shear stress below the yield stress value - short duration	43
3.34	Structure build-up with applying a shear stress below the yield stress value - long duration	43
3.35	Laponite - constant shear rate, 4000-1 (1/s)	44
3.36	Laponite - flow curve, 4000-1 (1/s)	44
3.37	Laponite - constant shear rate, 1-0.01 (1/s)	45
3.38	Laponite - flow curve	45
3.39	Laponite - flow curve, cloud of data points	46

3.40	Laponite - flow curve, trend line	46
3.41	Laponite - creep tests	47
3.42	Laponite - critical stress, flow in tube	48
4.1	Transient structure build up - break down tests	50

List of Tables

3.1	Crosshatched chart	21
3.2	Sandblasted chart	22
3.3	DIN Rotor and Standard Cup chart	23
3.4	Grooved Recessed-End Rotor and Grooved Cup chart	24
3.5	Technical features, WTPD-4010	26
3.6	Technical features, series 490	26

1

Introduction

Increased exploration and production from deepwater fields have brought up flow assurance issue to leading edge. Concerns about wax deposition and gelation play a significant role in deepwater and ultra-deepwater development projects. Water depth, long distances from the reservoir to a host facility via subsea and extended export pipelines in cold ambient water temperatures all pose risks for operators to note out when planning their development scenarios.

Wax deposition and gelation are two potentially catastrophic issues in crude oil and gas condensate systems. The deposition of n-paraffin will commonly occur along the pipe walls when the temperature of produced fluids falls below the Wax Appearance Temperature (WAT) or cloud point, at which the first wax crystals start to precipitate out of solution.

Wax gelation is less common in steady-state than wax deposition, but it can have even greater impact, if during production system shutdowns, fluid temperature drops below the fluid pour point, allowing the formation of a solid wax column. This situation can completely block the pipeline.

Gelled waxy crude oils often exhibit rheological behavior analogous to yield stress fluids. There is a critical or range of stresses, below which no flow occurs, but above which the viscosity of a gelled system decreases drastically. Thus, in order to restart flow of a gelled crude, a pressure larger than the typical operating pressure should be applied to exceed the yield stress of the fluid at wall [51, 107, 10].

The main aim is to determine the minimum pressure at the tube entrance to generate stress higher than its yield through gelled crude [39].

1.1 Scope of Thesis and Roadmap

To better comprehend the startup flow of gelled waxy crudes, the yield stress fluids could be studied as an analogy. This work is concentrated on exploring a concept of critical stress through experimental investigations using yield stress fluids.

For sake of this objective, some tests were designed to be performed using rheometer and experimental setup which simulates flow in tube condition, then it was aimed to connect and verify these results.

The roadmap in brief is as follows: to check the fluid flow in tube using Newtonian fluid considering compliance with hagen-poiseuille law and next to conduct tests using yield stress fluids. At this part a plan is digging into the

details of yield stress fluid characteristics using thixotropic and simpler one. The chapter three talks wholly about this experimentations.

The work begins using commercial hair gel as a simple yield stress fluid. The main experiments include flow curve and creep tests using rheometer, minimum pressure and pressure-rate measurements in experimental set up. Finally, the results were compared with appropriate non-Newtonian fluid model.

The same tests were carried out to discover the critical stress for Laponite suspension as a thixotropic yield stress fluid.

At the end, final discussion about the whole study is inserted.

2

Background of Study

At low temperatures it is possible for wax to precipitate out of the crude oil mixture and form gel-like structure [127, 128]. For example, in offshore oil production, long pipelines convey crude oil from a well head up to the platform. Shutdown of crude transport is often necessary, some times for long periods. Waxy oil leaves the well at nearly reservoir temperature, and then is exposed to much lower temperature of seawater. In these cases, gelation typically occurs, and the usual solution to displace the gelled crude is to pump another fluid (typically water or light oil) into the pipeline at high pressure [22, 132].

In order to grasp a subject of yielding of these gel structures during a pipeline restart flow, it is necessary to study the behavior of waxy crude oils at temperatures below the wax appearance temperature, which wax precipitates first begin to form in the mixture [129, 130].

Visintin and co-authors demonstrated that waxy crude oils exhibit a strongly temperature-dependent yield stress (σ_y) when they are below their wax appearance temperature. The yield stress is important in determining the applied pressure drop required for restart of a gelled pipeline.

2.1 Yield Stress Fluids

There is rheologically-complex materials that do not flow if the imposed stress is below some critical value, only it flows at stresses above this value. Experimentalists for a material with this property prefer the terminology of yield-stress fluids and the stress value that marks this transition is called the yield stress. The most usual rheological model for these materials is the Herschel-Bulkley model:

$$\text{for } \sigma > \sigma_y, \sigma = \sigma_y + K\dot{\gamma}^n \quad (2.1.1)$$

with σ being the stress, σ_y the yield stress and $\dot{\gamma}$ the shear rate; K and n are adjustable model parameters.

For a number of years there has been a controversy about whether the yield stress marks a transition between solid and liquid state, or a transition between two liquid states with very different viscosities [10, 77]. Numerous papers have been published that demonstrate these materials flow as very viscous Newtonian liquids at low stresses. Possibly the earliest work that seriously questioned the solidity of yield stress fluids below the yield stress is a paper by [7] where they show data on carbopol samples apparently demonstrating the existence of a finite viscosity

plateau at very low shear stresses-rather than an infinite viscosity below the yield stress. Following the initial publication by Barnes, a number of papers appeared discussing the definition of yield stress fluids, whether such things existed or not, and how to demonstrate them either way [11, 118, 49, 114, 54]. Due to outcome of this debate the rheology society at present holds two coexisting and conflicting views: (i) the yield stress marks a transition between a liquid state and a solid state and (ii) the yield stress marks a transition between two fluid states that are not fundamentally different-but with very different viscosities.

Over the last 20 years many methods have been developed for measuring yield stress, more than for any other rheological property [98, 34, 28, 59, 124, 46, 38]. While each method has its own merits and limitations [95], and although some techniques are more popular than others, none of them is accepted as the standard procedure for the determination of yield stress.

Yield stress fluids are then classified into two distinct types: thixotropic and non-thixotropic (or simple) yield stress fluids. A simple yield stress fluid is one for which the shear stress (and hence the viscosity) depends only on the shear rate, while for thixotropic fluids the viscosity depends also on the shear history of the sample [84].

The term thixotropy brought up by [100], the first paper that properly described the phenomenon. This combines the Greek words thixis (stirring or shaking) and trepo (turning or changing). However, [106] soon afterwards stated that the true meaning of thixotropy was 'an increase of viscosity in a state of rest and a decrease of viscosity when submitted to a constant shearing stress'. Thixotropy is generally understood as the time-dependent decrease in the viscosity of a fluid due to a finite, measurable, reversible change of the fluid microstructure during shear; this mechanism is commonly referred to as shear rejuvenation. In the absence of shear, generally a damaged structure rebuilds, i.e., it is said to age. All liquids with microstructure can show thixotropy, can move from any one state of microstructure to another and back again, whether from different states of flow to rest and vice-versa [9].

The true steady-state behaviour of a thixotropic fluid is seen both after an infinite shearing time at any shear rate or shear stress applied or infinite rest time. Of course, as all these equilibrium states are approached asymptotically, one comes close to this state after a reasonable rather than an infinite time, but even then, breakdown times of hours and rebuilding times of days might be necessary to fully describe a very thixotropic system [9].

One method that has been frequently used for characterizing yield stress materials is to work with two yield stresses-one static and one dynamic [91]. The static yield stress is the stress above which the material turns from a solid state to

a liquid one, while the dynamic yield stress is the stress where the material turns from a liquid state to a solid one [9, 81].

2.2 Wall Slip

Wall slip can play an important role in the context of waxy crude oil rheology [73]. Kind of shear heterogeneity which was first studied by [88]. Wall slip is a complex phenomenon to which many physical and chemical factors contribute [116].

In a flow of viscous fluids over solid surfaces, the 'no-slip' at fluid-solid interface is a widely-accepted boundary condition with strong experimental support. Violations of this condition are widely recognized in many situations, especially in the flow of non-Newtonian fluids. Wall slip could lead to large errors and hence complicates the analysis of fluid systems and introduces serious practical difficulties [67, 96].

Stokes was the first to adopt the no-slip as a general condition at the boundary of solid surfaces [37, 75]. The no-slip condition is experimentally verified in numerous cases by direct observation and by deduction through its inevitable consequences [2, 93]. Similarly, the slip at wall is confirmed in a large number of experimental studies [29, 102, 35, 82, 92, 79]. However, most often it is detected indirectly through its effects on the flow [79, 16, 47].

There are several signatures that reveal the occurrence of slip in various rheological and fluid transport systems. One of these signatures is the dependence of rheological properties, like viscosity, on flow geometry such as a gap width in parallel plate rheometers or shape and radius of capillaries [76, 24, 61, 79, 71, 63, 8, 52, 109, 25, 95, 4, 131, 97, 14, 83].

Another signature of wall slip is an influence of composition of the surface and its physicochemical characteristics such as wettability and roughness on the rheological and flow properties [71, 131]. A third signature, which is specific to yield stress materials, is disappearance of yield-stress or a drop in the yield stress value [104, 119].

There is no general theory to describe wall slip in all situations. There are number of mechanisms proposed to explain slip in certain circumstances [75]. One of these mechanisms is the depletion of boundary layer where particles in a sheared dispersed system, such as emulsions and suspensions, migrate away from the boundary region resulting in a very thin low viscosity layer adjacent to the wall which acts as a lubricating film that facilitates fluid movement [8, 29, 4, 76, 13, 72, 112, 117, 63, 3, 25, 31, 57, 108, 50, 126, 5].

Another proposed mechanism for wall slip is development of a layer of

adsorbed particles on the solid surface due to strong attractive forces between these dispersed particles and the surface. This layer acts as a 'soft cushion' over which the particles in fluid slide [115].

In the literature of rheology and fluid mechanics, wall slip is divided into 'true slip' where there is an adhesive failure at the interface, and 'apparent slip' where there is an inhomogeneous thin layer of fluid adjacent to the wall with different rheological properties to the bulk of fluid which facilitates fluid movement [64, 75, 70, 134, 23, 15, 52, 135, 3, 63, 57]. The 'apparent slip' designation comes from the fact that large velocity gradients across the very thin low-viscosity slip layer give an impression of slip at wall although the nonslip condition is not violated [62, 31, 8]. Generally, the apparent slip becomes more pronounced as the viscosity of the slip layer relative to the viscosity of bulk of fluid decreases [63].

Both true and apparent slip have been confirmed experimentally [56, 80, 8, 31, 101]. In most cases true slip is not the cause of tangible macroscopic slip. The reason is that the presence of wall roughness, as a minimum at microscopic and sub-microscopic levels and molecular forces between the fluid and solid, hinders substantial movement of the fluid at the interface. Therefore, apparent slip, rather than true slip, is the more common and viable mechanism for the observable wall slip [112]. Even in the case of yield-stress fluids where slip occurs before bulk yielding while the material is still solid, slipping usually occurs through a very thin boundary layer of the fluid where stress in this region exceeds the value of yield-stress or through a film from the fluid phase or from an alien phase.

2.3 Wall Slip and Yield Stress Fluid

Wall slip is commonplace in yield-stress fluids. One of its consequences is an apparent yield due to slip at lower stress than the bulk yield-stress. This apparent flow due to slip obscures the true yield-stress behavior of material [109, 63, 108, 74, 111]. In this situation, possibly the local stress is below the yield value except at the boundary region. So, yielding occurs only at a very thin layer adjacent to the surface, which serves as a lubricating slip film [115, 104, 133, 119, 59, 131]. In these cases, direct observation techniques, such as visualization, may be required to clarify the situation [78].

There is also the possibility that sliding occurs through a depleted inhomogeneous layer from the continuum phase, or through a film from another phase which exists on the surface prior to the contact or is deposited on the surface from the bulk phase [95, 105].

Slip can also lead to large errors in viscosity estimations and flow rate predictions in these systems [79, 115, 63, 104, 78, 111]. The dependence of this

behavior on factors, such as rheometric geometry and surface conditions, would reveal that it is arising from slip.

In an experimental study on the flow of highly concentrated suspensions of soft particles, it has been reported by [79] that depending on the value of applied stress three regimes of slip have been detected: at low stress (below yield stress) the flow is entirely due to wall slip, slightly above the yield-stress both bulk flow and slip have significant contribution to the fluid motion and well above yield stress the slip is negligible and the flow is almost entirely due to bulk deformation. Similar observations have been reported in other studies [115, 111].

2.4 Slip Control

In practical situations where wall slip is unwanted, various methods are employed to eliminate or minimize slip, although total elimination could sometimes be very difficult or even impossible to achieve [23]. For example, surfaces are deliberately roughened to reduce the effect of slip [80, 71, 8, 72, 115]. This is achieved by various techniques such as serrating, coating, impregnating the surface, abrasive blasting, chemical treatment or attaching solvent-proof sandpapers [115, 27, 104, 23, 63, 3, 8, 20, 78, 74, 95, 131, 97, 26, 111, 40]. Some of these techniques could disturb the system by introducing or modifying other factors than affect slip [93]. Also, excessive roughness may induce turbulence and instabilities [99, 45].

The effect of roughness on wall slip is a controversial issue with quantitatively and qualitatively contradicting findings [93, 35, 108]. Various proposals have been put forward to explain the effect of roughness on slip in different systems and under various circumstances. For example, one proposal is that roughness disrupts or prevents the formation of a depleted layer [97, 47]. In this regard, it has been argued by [123] that for roughness to be effective by disrupting the depleted slip layer, the roughness profile must be larger than the thickness of this layer. Roughness is normally quantified by giving the average (or root mean square) height of the roughness peaks or the depth of grooves [80, 53, 42, 105], or by giving the peak-to-peak mean distance [12, 33].

The effect of roughness has also been explained by an idea that on atomic scale, it increases the fluid-solid interaction through an increase in the contact surface [17].

Slip can also be controlled by changing the physicochemical properties of the surface other than roughness, such as wettability, through chemical treatment or surface coating or by choosing a proper type of material [75, 29, 102, 115, 55, 104, 8, 31, 53, 131, 50, 125, 60, 113]. Another means to eliminate or reduce wall slip is to increase surface to volume ratio, although this could complicate the measurement

procedures and may not be practical in some circumstances due to experimental restrictions [21, 95].

3

Experimentation

3.1 Rheometry

An important component of the study of complex fluids is rheometry, which broadly encompasses the development of specific experimental techniques and quantitative measurements for characterizing the rheology of a particular material.

3.1.1 The AR-G2 Magnetic Bearing Rheometer

TA Instruments rheometer, the AR-G2, was launched in February 2005. Two features were introduced for this instrument to provide a low torque performance never previously obtainable on a commercial rheometer. Good low torque performance is important for the rheological characterization of soft materials. The broader a rheometer torque range, and the better its operation at the low torque end of the range, the more fully and accurately the rheological properties of these materials can be measured.

The AR-G2 is a combined motor and transducer (CMT) instrument. This design has traditionally been used for rheometers like the AR-G2 that operate in controlled stress in their native mode. The lower component of the measuring system is fixed, the upper component is attached to a shaft, that can rotated by a torque produced by an induction motor (See Fig. 3.1).



Figure 3.1: Rheometer AR-G2

The constraint on the low torque performance of such an instrument is the friction between rotating and stationary components. An induction motor is

therefore used not only because the rapidity and stability of its response, but more specifically to minimize the friction.

But the rotating shaft has to be supported in some way, and this requires a bearing: another source of friction. Until now, all high performance commercial CMT rheometers have used air bearings, either of the jet or the diffusion type, and for progress to be made, a new technology had to be found : a magnetic bearing, which had previously been used for research instruments used only in creep [103].

The move from air to magnetic technology greatly reduced the friction from the bearing itself, but to make full use of this improvement, it was also necessary to make changes to the motor, to reduce the friction due to that component of the rheometer. To do this, the gap between the stationary and the rotating component was increased.

It was important that the improvements in the low torque performance produced by the changes to the motor and bearing should not have been achieved at the expense of performance elsewhere, in particular by reducing the instrument stiffness or substantially increasing the inertia. But checkout process demonstrate that the improvements have been made without compromising on the rheometer's mechanical stiffness or its inertia [32].

3.1.2 Geometries

Peltier Plate Geometries

Peltier Plate geometries come in 8 mm, 20 mm, 25 mm, 40 mm, 50 mm, and 60 mm diameters. Upper Cone geometries are available in 0.5°, 1°, 2°, and 4° cone angles. By changing diameter and cone angle, the measurable range of stress and strain or shear rate can be varied to capture the widest range of material properties [44, 43].

Standard Peltier Plate The Standard Peltier Plate is the most common selection, offering an 80 mm diameter hardened surface to accommodate up to 60 mm upper plates for maximum sensitivity [44, 43].

Materials of Construction and Surfaces Peltier Plate geometries come standard in the following materials:

- Stainless Steel: Rugged, very good chemical resistance for highly basic or acidic materials

- Stainless Steel with Composite Heat Break: Same properties as stainless steel with added benefit of composite heat break, which insulates upper geometry when controlling temperatures away from ambient
- Hard Anodized Aluminum: Excellent thermal conductivity, low mass, fair chemical resistance
- Titanium: Low mass, excellent chemical resistance

Geometries are available in multiple surface finishes, including smooth, sandblasted, and crosshatched [44, 43].

Crosshatched

About characteristics of Crosshatched geometry notice Table. 3.1.

Table 3.1: Crosshatched chart

Diameter	Roughness	Gap
60 mm	500 microns	1000 microns

See figures (3.2, 3.3) for more on this.



Figure 3.2: Crosshatched plate

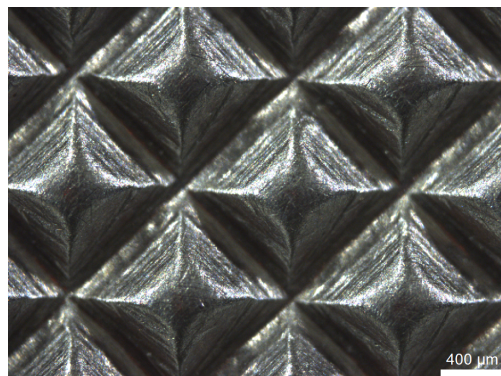


Figure 3.3: Crosshatched roughness

Sandblasted

About characteristics of Sandblasted geometry notice Table. 3.2.

Table 3.2: Sandblasted chart

Diameter	Roughness	Gap
60 mm	1.25 microns	500 microns

See figures (3.4, 3.5) for more on this.



Figure 3.4: Sandblasted plate



Figure 3.5: Sandblasted roughness

Cup and Rotor Geometries

The standard Peltier Concentric Cylinder geometries include a cup radius of 15 mm, configured with either a Recessed End or DIN Rotor. Both rotors have a radius of 14 mm and height of 42 mm. The double gap concentric cylinder has an additional shearing surface over single gap providing lower stress and higher sensitivity for extremely low viscosity solutions [44, 43].

Special Cups and Rotors Specialty geometries include various vanes, helical, and starch pasting impeller rotors, as well as large diameter and grooved cups. These special concentric cylinder geometries are very valuable for characterizing dispersions with limited stability, preventing error from slip at the material/geometry interface, and for bulk materials with larger particulates. Vane geometries are available in both a 14 mm and 7.5 mm radius. The large diameter cup has a radius of 22 mm. The helical and impeller rotor and cup keep a sample mixed or particles suspended during shearing [44, 43].

DIN Rotor and Standard Cup

About characteristics of DIN Rotor and Standard Cup geometry notice Table. 3.3.

Table 3.3: DIN Rotor and Standard Cup chart

Rotor Diameter	Cup diameter	Operating Gap
27.97 mm	30 mm	5900 microns

See figures (3.6, 3.7) for more on this.



Figure 3.6: DIN Rotor



Figure 3.7: DIN Rotor and Standard Cup

Grooved Recessed-End Rotor and Grooved Cup

About characteristics of Grooved Recessed-End Rotor and Grooved Cup geometry notice Table. 3.4.

Table 3.4: Grooved Recessed-End Rotor and Grooved Cup chart

Rotor Diameter	Cup diameter	Operating Gap
27.66 mm	30 mm	3600 microns

See figures (3.8, 3.9) for more on this.



Figure 3.8: Grooved Recessed-End Rotor

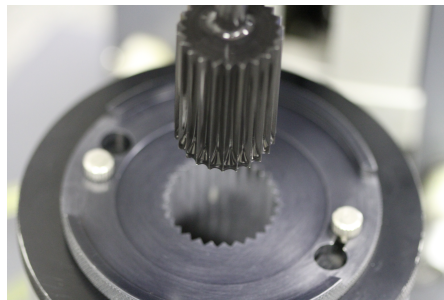


Figure 3.9: Grooved Recessed-End Rotor and Grooved Cup

3.2 Fluid Transport in Tube

3.2.1 Experimental Setup

Experimental setup is established to investigate and characterize the flow of fluid in tube. The setup consists of a reservoir with maximum volume of 4.7 liter, a roughened snaked-like tube with length of 2.5 meter and radius of 1 cm, manometers and some connections.

Tube

Two plates each containing snaked-like semi-circle tube together form the tube in this setup. Aforesaid structure provides an opportunity to have an access to the tube wall to alter the roughness if it is needed. The structure is illustrated in figures (3.10, 3.11) more detailed.

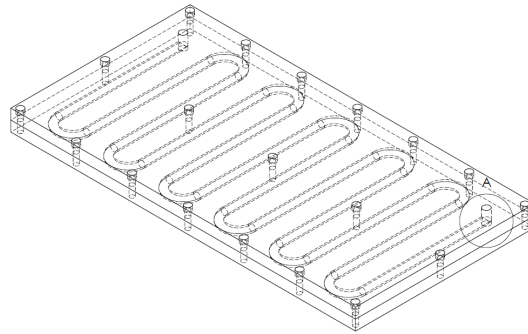


Figure 3.10: Bolted plates enclosing a snaked-like tube

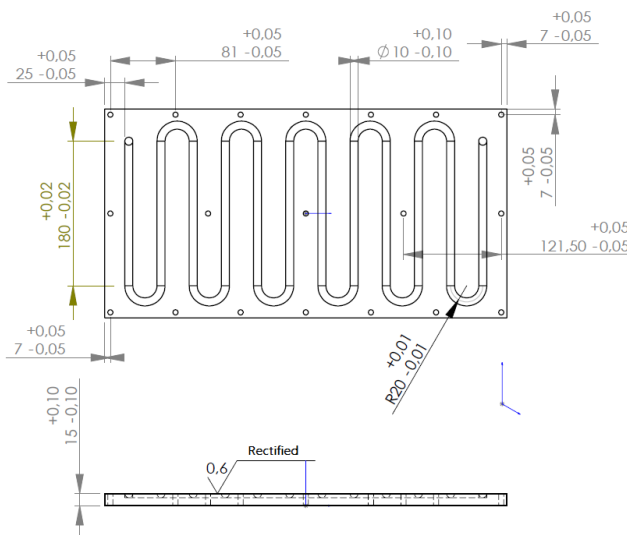


Figure 3.11: Top and side view of single plate containing semi-circle tube

Differential Pressue Measurement

Depending on a range of differential pressure, two different types of manometers were used.

WTPD-4010 Differential pressure transmitters For pressures below than 1 bar this transmitter was used (See Fig. 3.12). WTPD-4010 differential pressure transmitters have resistive piezoelectric sensor element which convert a pressure

difference between high and low side exerted by fluid to an electrical signal, the electrical signal is amplified, linearized and made available in standardized sign. For more technical data notice Table. 3.5.

Table 3.5: Technical features, WTPD-4010

Feed	9-33 V DC
Accuracy	$\pm 0.25\%$ FS
Temperature Limit	0 to 70° C



Figure 3.12: Manometer for pressures less than 1 bar

Series 490 Digital Manometers For pressures over 1 bar this type of manometer was used (see Fig. 3.13). Series 490 Digital Manometers are versatile, hand-held, battery operated manometers available in several basic ranges. All models measure either positive or negative differential pressures with $\pm 0.5\%$ of full scale accuracy. For more technical data notice Table. 3.6.

Table 3.6: Technical features, series 490

Feed	9 Volt alkaline battery
Accuracy	$\pm 0.5\%$ FS
Pressure Hysteresis	$\pm 0.1\%$ of FS
Temperature Limit	0 to 40° C



Figure 3.13: Manometer for pressures larger than 1 bar

Another component of the setup is connections which assemble the whole together.

Applying air pressure, fluid flows from reservoir through manometer and tube, therefore the transport of fluid into tube could be examined. Figure (3.14) shows the whole experimental setup.

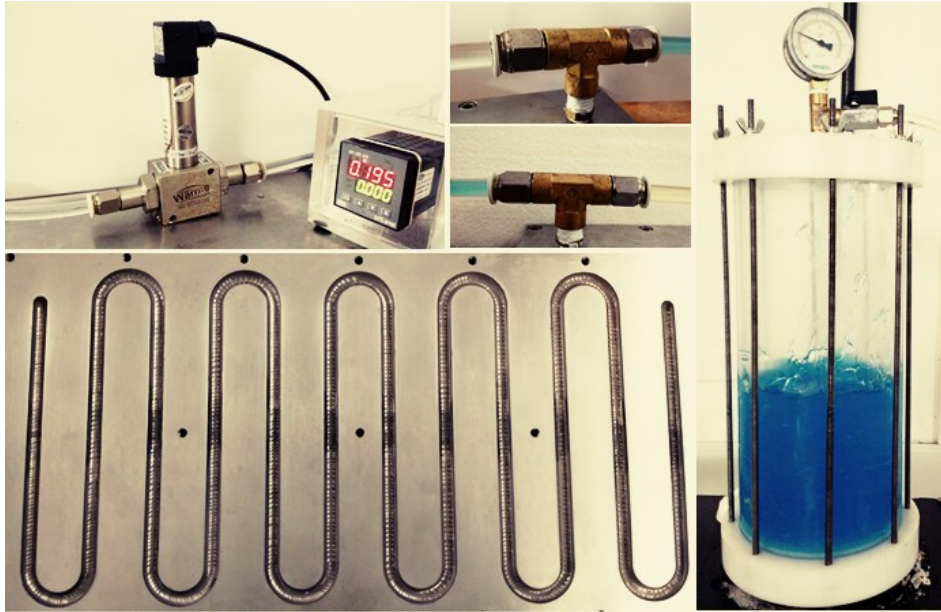


Figure 3.14: Experimental setup - fluid transport in tube

About the wall roughness of tube, it should be mentioned that different tests were performed until a sufficient roughness was achieved which consequently slip was totally eliminated. The roughness is not quite uniform through the whole tube and it varies in the range between 1 to 400 microns but the 100 microns is a totally acceptable average value as R_a of roughness at tube's wall. For more insight about shape of roughness at the tube's wall figure (3.15) is inserted here.

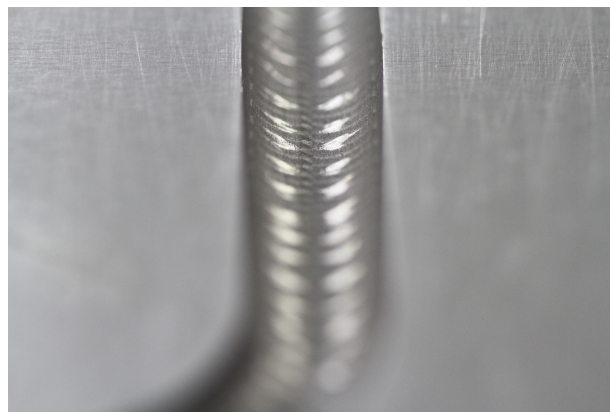


Figure 3.15: Wall roughness along tube

As it is discussed before the experimentation will be conducted using three different fluids; Newtonian, simple yield stress and thixotropic yield stress fluids, let us begin with Newtonian fluid. It should be mentioned that all tests during this work are performed at room temperature of 25 °C.

3.3 Newtonian Fluid

The main objective of this part is to verify the fluid transport through the established experimental setup or in better words, if the Newtonian fluid transport through the tube satisfies Hagen-Poiseuille law or not.

Hagen-Poiseuille law is a physical law that gives the pressure drop in an incompressible and Newtonian fluid in laminar flow through a long cylindrical pipe of constant cross section [120].

$$\Delta P = \frac{8\mu LQ}{\pi r^4} \quad (3.3.1)$$

where:

ΔP is the pressure loss, μ is the dynamic viscosity, L is the length of pipe, Q is the volumetric flow rate, π is the mathematical constant Pi, r is the radius.

The tested Newtonian fluid is 99.5% Glycerol with chemical formula of $C_3H_8O_3$ and density of 1.25 gr/ml.

The following figure (3.16) shows the viscosity of Glycerol at different temperatures.

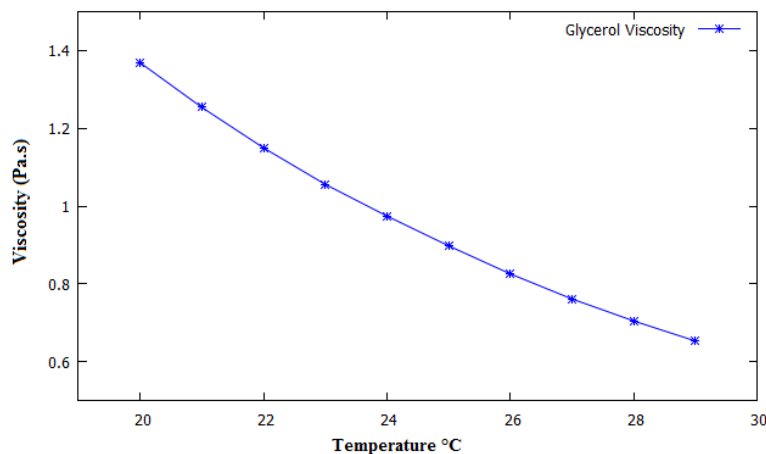


Figure 3.16: Glycerol viscosity

A procedure is to exert various pressures at the reservoir containing Glycerol and measuring a resultant flow rate through the tube. Temperature in whole process is monitoring, so at any temperature the proper viscosity for glycerin is available. In addition, the length of tube is known from design data, also the viscosity and density of fluid, the pressures and flow rates are measured, so radius

could be calculated. This measured radius would be compared with the value for radius in hand from design info to see that if the calculated radius is satisfactorily close to that of geometrical one.

Here is the experimental data for the calculated radius which is result of eight different pressure-flow rate measurements (See Fig. 3.17).

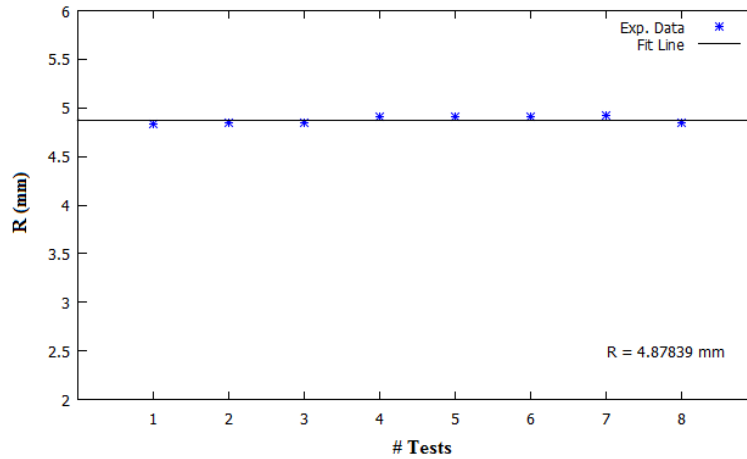


Figure 3.17: Calculated radius using Hagen-Poiseuille law

The geometric radius value is 5 mm and the calculated one is 4.88 mm which regarding errors in measuring flow rate, is satisfactory with good precision.

As the most important result of this whole process, it shows the all part of experimental setup specially the measurement apparatus are brought together properly.

3.4 Simple or Thixotropic?

This part belongs to study of yield stress fluids, but at the beginning, some rheometric tests are introduced here to show what does it mean a simple or thixotropic yield stress fluids in more tangible way.

In this study commercial hair gel was used as a simple yield stress fluid and 2 % aqueous suspension of Laponite as a thixotropic yield stress fluid. More detailed info about characteristics of these fluids will be given later through this chapter.

First set of tests points out an effect of time and structure breakdown as a shear history. Different shear rates were applied step-like to the fluids in an Ascending Order and then the same ones in a descending order. Every step lasts 2 minutes for hair gel and even more, 5 minutes for Laponite suspension.

Figures (3.18 and 3.19) shows resultant shear stresses versus time.

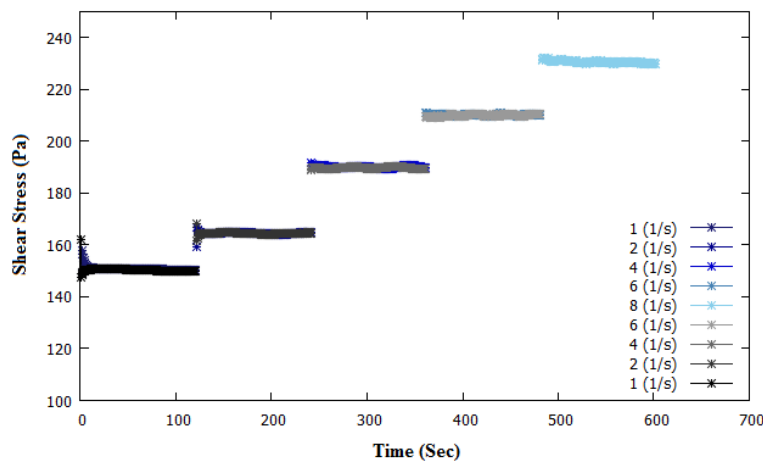


Figure 3.18: Commercial hair gel - thixotropy, Test 1

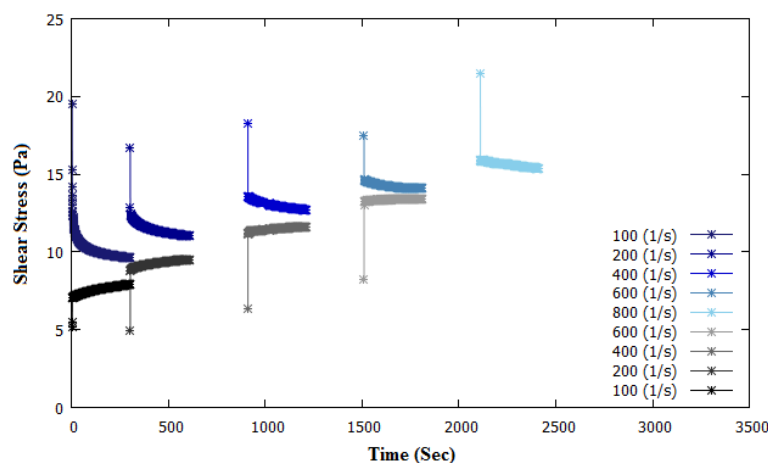


Figure 3.19: Aqueous solution of Laponite - thixotropy, Test 1

Results underline that for hair gel, the resultant shear stresses are almost the same in both ascending and descending orders except in low shear rates which

needs a little bit more time. Besides for Laponite suspension (that for each step possesses even more time), it is obvious that takes lot more time to reach the same value for each shear rates.

Figures (3.20 and 3.21) help to evaluate the effect of time and structure build up. In this set of tests fluids undergo constant shear rate steps and between each one there is a rest period (putting fluids under very low shear stress ensuring below the yield one) with different durations.

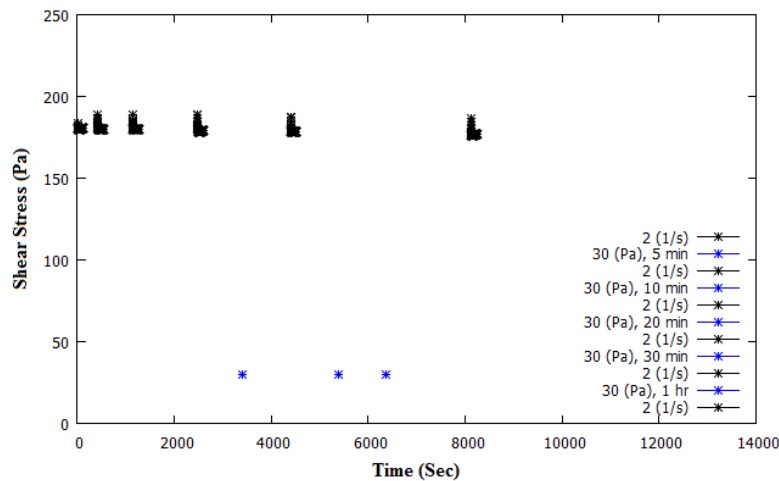


Figure 3.20: Commercial hair gel - thixotropy, Test 2

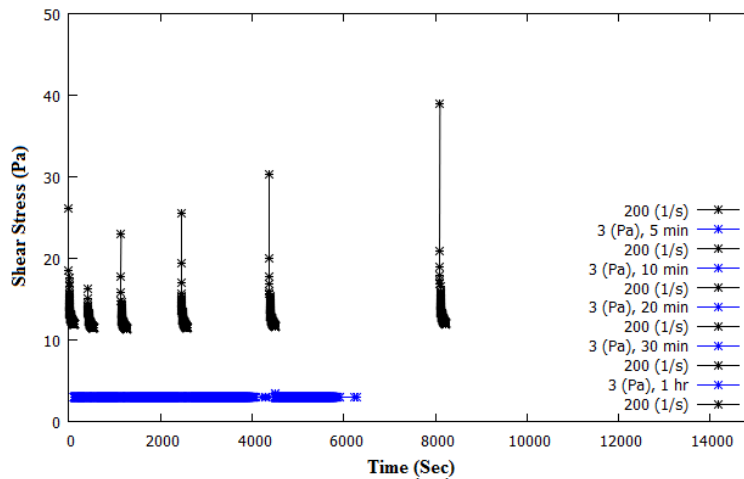


Figure 3.21: Aqueous solution of Laponite - thixotropy, Test 2

For hair gel after each rest step, shear stress starts from almost the same value. For Laponite solution, shear stress begins with different measures and the larger the rest time, the greater the first shear stress point which proves signature of structure build up.

So regarding these tests, this could be understood that for hair gel influence of time and shear history is almost negligible comparing with Laponite solution

however, there is such an effect but much less. Therefore hair gel could be considered far simpler than thixotropic Laponite suspension.

3.5 Simple Yield Stress Fluid

Discovering the minimum pressure or the critical shear stress above which fluid flows is a main objective of the study in this part. As aforesaid, a commercial hair gel (gel Bozzano - mega forte 4) was used as a simple yield stress fluid through this experimentation (See Fig. 3.22).



Figure 3.22: Rheometric tests - hair gel

First step is to assure no slip condition. A flow curve test was run using different rheometric geometries, smooth plate and two others; crosshatched and sandblasted which have roughened surfaces (See Fig. 3.23).

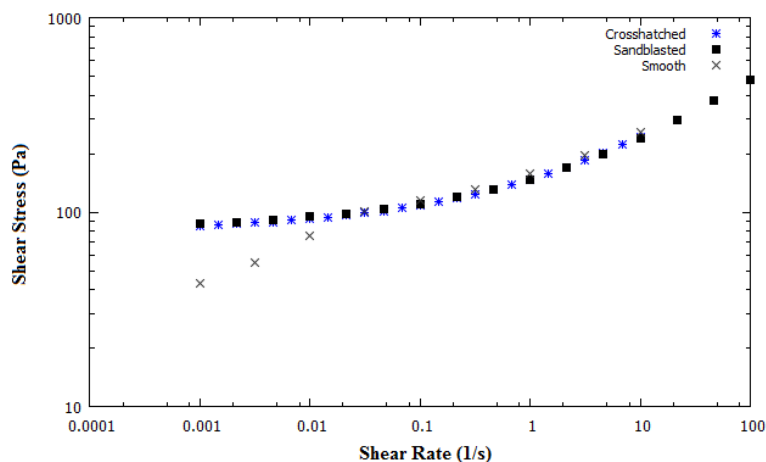


Figure 3.23: Flow curve - hair gel

As discussed before, one signature of wall slip is a drop in yield stress value which could be seen in data of smooth geometry. Another signature is the dependence of rheological properties on the flow geometry such as the gap width

in parallel plate or on the composition of surface like roughness. Two different geometries with distinct R_a and operational gaps were tested in this experiment and as illustrated in the graph, shear stress values at any shear rate is mostly the same for both ones which is a definite sign of no-slip condition for these two geometries: crosshatched and sandblasted.

One of the most reliable methods to measure critical shear stress is conducting creep test. That is to say exerting different shear stresses from very small one in ascending order through defined period of time to observe at which shear stress value the fluid starts flowing, this minimum shear stress is equivalent to static yield stress. One hour is selected as a test duration and is kept constant through the whole study (See Fig. 3.24).

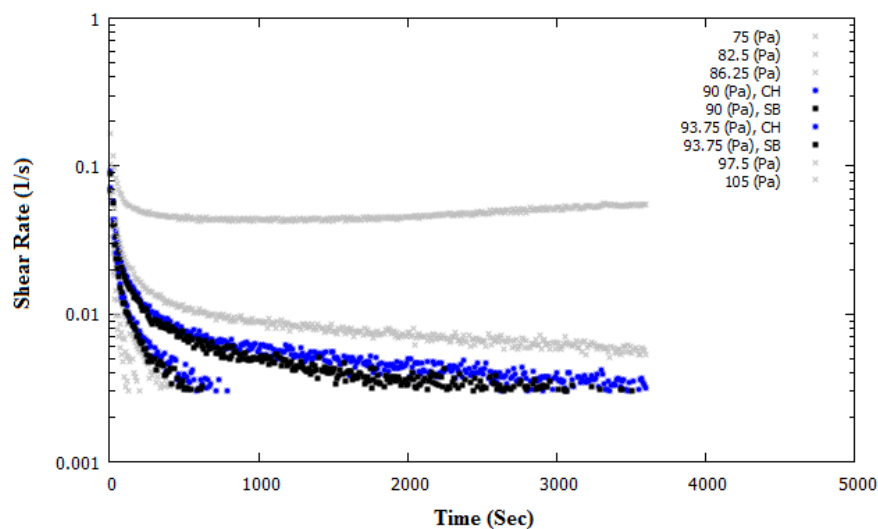


Figure 3.24: Creep flow test - hair gel

The all tests were carried out using crosshatched geometry but for two marginal ones; 90 Pa and 93.75 Pa; were repeated using both cross hatched and sandblasted plates.

Due to the results ' 93.75 Pa ' is the critical shear stress which hair gel begins to flow.

At this point, same tests should be performed in experimental setup; calculating minimum pressure for fluid transport through tube. Different pressures were put on reservoir from very small one with duration of one hour, if did not flow, pressure was increased a little bit till finding the minimum pressure which hair gel starts to flow through tube.

This minimum pressure was recorded as 1.07 bar for hair gel. Now a tool is needed to translate this minimum pressure to an equivalent critical stress.

Shear stress at the wall can be calculated directly by the balance of pressure and frictional forces:

$$\sigma_w = \frac{r}{2} \frac{\Delta P}{L} \quad (3.5.1)$$

Where r is an effective radius of the tube to fluid, ΔP is differential pressure over inlet and outlet of the tube and L is length of the tube.

The critical stress evaluated through tube should be compared with that of measured at rheometer to ensure there is no slip at tube wall. Effective radius of tube to yield stress fluid is needed but first calculations were done applying radius measured using Newtonian fluid as guideline which gives $\sigma_w=101.16$ Pa. This value is larger than what measured in rheometer, so it is acceptable.

To calculate effective radius of tube to non-Newtonian fluid, regarding there is non-slip condition in both rheometer and tube, therefore the yield stress value is so properties of material and it should be the same at any fluid flow geometry. Then the effective radius could be calculated as:

$$93.75 Pa = \frac{r}{2} \frac{107000 Pa}{2580 cm} \quad (3.5.2)$$

and $r = 4.521$ mm.

This part will be accomplished if for any flow rate demanded, the required pressure be known. As explained before, the most usual rheological model for simple yield stress material is the Herschel-Bulkley. The objective is to cross-check and verify the experimental results with Herschel-Bulkley exact solution.

For some differential pressures larger than the minimum pressure, related flow rates were measured. For Herschel-Bulkley [Eq. (2.1)] solution K and n ; an adjustable model parameters are needed.

Three flow curve data of hair gel were used to calculate best averaged k and n (See Figs. 3.25, 3.26, 3.27).

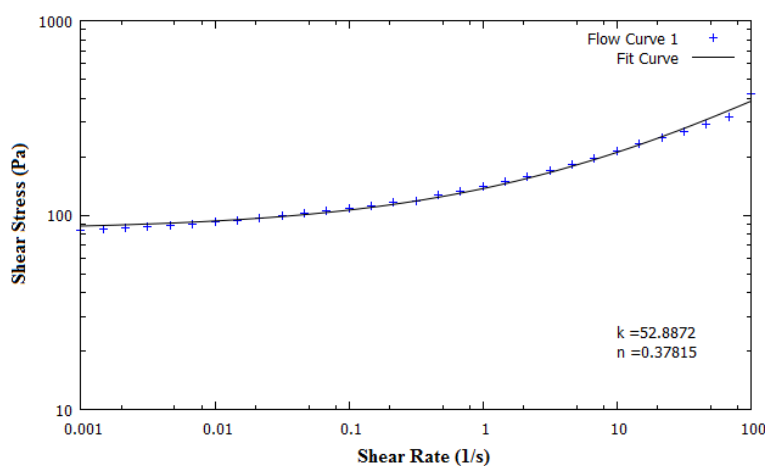


Figure 3.25: Flow curve 1 - hair gel

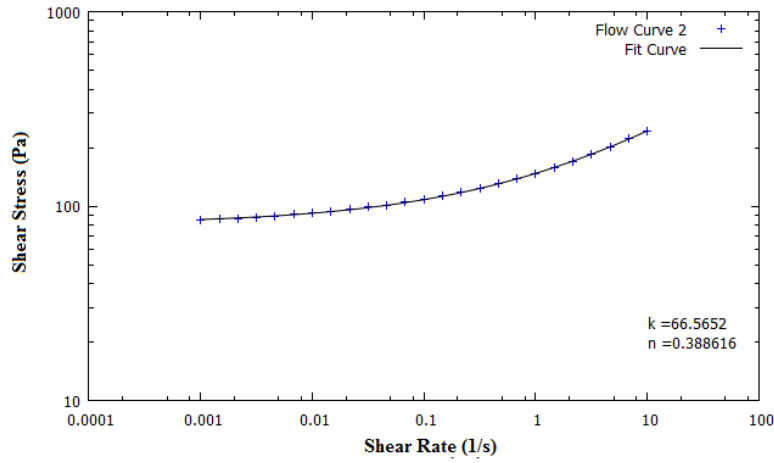


Figure 3.26: Flow curve 2 - hair gel

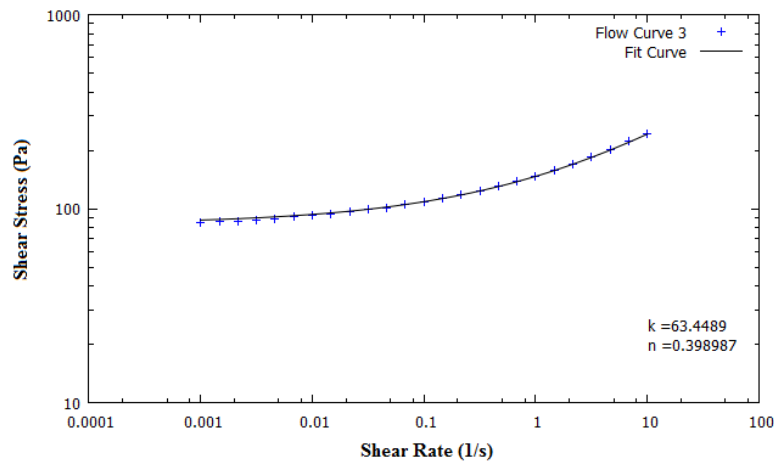


Figure 3.27: Flow curve 3 - hair gel

The calculated averaged values are $K = 60.9669$ and $n = 0.38859$.

Now results are compared in figure (3.28) where

$$\dot{\gamma}_1 = \left(\frac{\sigma_y}{k}\right)^{\frac{1}{n}} \quad (3.5.3)$$

. The axes are dimensionless parameters of velocity versus shear stress.

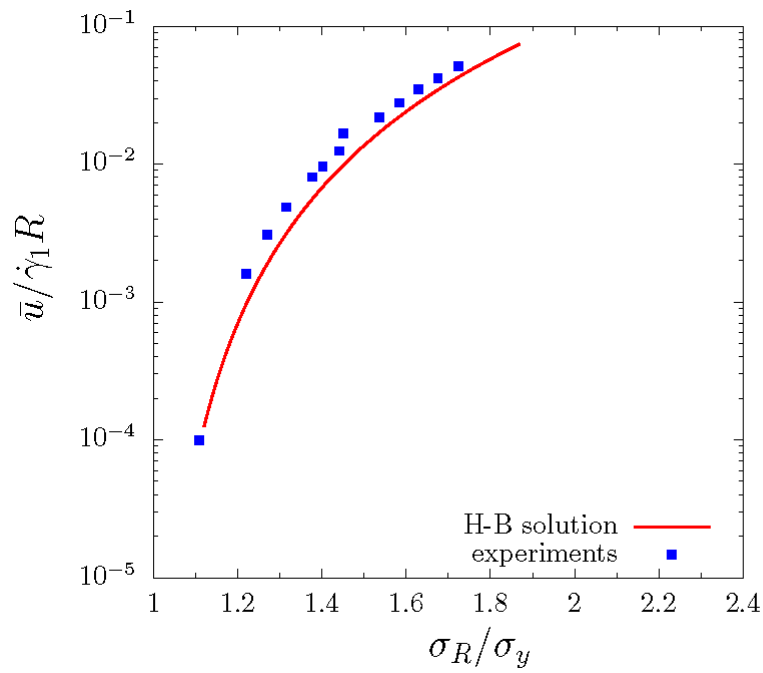


Figure 3.28: Experimental data and Herschel-Bulkley solution

This points out an almost perfect match of experimental pressure-flow rate data in tube with Herschel-Bulkley solution. This matching asserts that the procedure is quite satisfactory and the objective of combining rheometric and fluid transport knowledge is fully achieved. In continuation this procedure is kept on.

3.6 Thixotropic Yield Stress Fluid

Laponite (hydrous sodium lithium magnesium silicate) is a synthetic crystalline layered silicate colloid with crystal structure and composition closely resembling the natural smectite clay hectorite. The experiments were performed on Laponite RD, a synthetic clay manufactured by Rockwood Additives Ltd. Its chemical composition is as follows: SiO₂, 65.82% ; MgO, 30.15% ; Na₂O, 3.20% ; Li₂O, 0.83% and corresponds to the chemical formula $Si_{8.00}(Mg_{5.45}Li_{0.40})H_4O_{24}Na_{0.75}$ and density ρ is around 2.65 gr/cm^3 [1, 36, 121].

The particles of Laponite are colloidal disks of 25 nm diameter and 1 nm thickness, with negative surface charge on both faces [65].

When Laponite is dispersed in water, the exchangeable sodium ions hydrate, causing the clay to swell initially and to separate completely. This gives a clear colloidal dispersion of anionic Laponite platelets and hydrated sodium ions in solution (See Fig. 3.29). The synthetic colloid Laponite exhibits an array of different phases and behaviors due to both attractive and repulsive interactions, anisotropy and net charge, as well as an anisotropic charge distribution [36, 48].



Figure 3.29: Rheometric tests - aqueous Laponite suspension

Many authors; [89, 90, 110, 121, 87] studied states diagrams of Laponite dispersions as a function of Laponite concentration and the concentration of added salt.

Figure (3.30) is reproduced from a work by [110] which describes phase diagram of Laponite suspensions with 4 regions:

- IL - Isotropic liquid phase
- IG - Glass (gel) phase
- NG - Nematic gel
- Flocculation (F)

Diagram shows that, at relatively low salt concentration and increasing clay weight, one can obtain an isotropic liquid phase (IL), a gel (or glass) phase (IG) and a nematic gel (NG), at high salt concentrations, one instead observes flocculation (F).

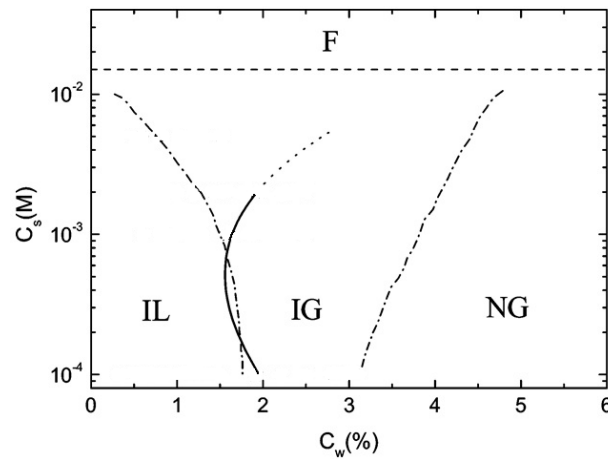


Figure 3.30: $C_s - C_w$ Phase diagram of Laponite solution

The rheological properties of Laponite dispersion are known to change over time. The aging period could be as long as a year. However the major changes take place during the first 7 days after their preparation [69].

In this study 2% clay concentration with 10^{-3} M salt concentration was chosen for the Laponite solution to obtain gel phase with desired range of yield stress value. Then the suspension was aged for 8 days before each test. The pH value of the suspension was fixed at 10 by addition of NaOH solution, thereby providing chemically stable particles [122, 90].

3.6.1 Preparation Scheme

some Bibliography

[18] - Suspensions of Laponite are prepared by dissolving the white powder at 3.5 wt % in ultrapure water (Milli-QPlus) under vigorous stirring for at least 15 min at pH 10. The pH is adjusted using reagent grade NaOH; working at high pH is necessary in order for the particles to be chemically stable.

[19] - We suspend the Laponite at a concentration of 3 wt% in ultra pure water (with NaOH to obtain a pH 10) under vigorous stirring during 15 min and subsequently pass the solution through a Millipore Millex AA (0.8 mm) filter, to obtain a reproducible initial liquid state.

[68] - All dispersions analyzed were done at a fixed pH of 10. Clay powder was mixed in a solution of demineralized water with a specific quantity of NaCl (in

order to fix the ionic strength) and sodium polyacrylate. Dispersions were prepared at room temperature and brisk stirring for 30 min.

[69] - The clay powder was vigorously dispersed for 30 min in a NaOH 10⁻⁴ mol/L solution. After added at room temperature and the vigorous stirring was continued for another 30 min. Dispersions were analyzed by rheometric and acoustic measurements 7 days after their preparation.

[66] - Laponite RD, synthetic hectorite clay was procured from Southern Clay Products, Inc. Laponite as white powder was dried for 4 h at 120 °C before mixing with ultra pure water at pH 10 under vigorous stirring. Basic pH, maintained by the addition of NaOH, provides chemical stability to the dispersion. The dispersion was stirred vigorously for 1 h by Ultra turrax T25 at a speed of 9500 rpm. The sample used to carry out RI measurement was filtered through a Millipore Millex-HV 0.45 micrometro filter unit.

To prepare Laponite RD solution, the Laponite powder should be baked to remove any moisture, adequate amount of ultra pure water be provided and solutions of NaOH and NaCl got to be prepared with pre-defined concentrations.

Whole procedure is presented here in detail:

Baking Laponite RD

To remove moisture,

- put the Laponite RD powder under 120 °C for 4 hours
- after the heating period, shake the bottle vigorously and then open the cap to vent the aerosols, repeat this procedure for 5 minutes
- close the bottle cap and leave it at rest for 1 day

NaCl Solution Preparation

23.4 gr of NaCl is demanded to make 1L of 0.4 $\frac{mol}{L}$ NaCl solution. The scheme is presented here step by step:

- dissolve weighted NaCl with ultra pure water till 900 ml of solution
- stir the solution with a rod in the beaker
- displace the solution to a volumetric flask with the funnel
- then wash the beaker and the funnel with ultra pure water into flask
- increase the final volume of the solution with ultra pure water to 1L
- plug the flask and shake it till turn into a homogeneous solution
- transfer the final solution to a plastic container

NaOH Solution Preparation

Procedure is as follows: 1.6 gr of NaOH is needed to prepare 1 L of 0.04 $\frac{mol}{L}$ NaOH solution

- dissolve this amount of NaOH with 400 ml ultra pure water
- and then add ultra pure water into beaker till volume reaches to 900 ml
- next, mix the solution with stirring rod
- transfer the solution to a 1 L volumetric flask with the funnel
- wash the beaker and the funnel with ultra pure water
- raise the volume of solution in the volumetric flask with ultra pure water until the absolute 1L
- seal the flask and rock it till ensure the solution is entirely homogeneous
- eventually, displace the prepared solution to a plastic container

Laponite Solution Preparation

To prepare 4 L of 2% wt Laponite solution,

- 110 ml of NaOH solution was diluted with 3800 ml of ultra pure water to maintain the PH at very close to 10
- prepare mixer with 3-bladed propeller, common impeller for axial and large circulating flow
- put the solution into mixer
- start the mixer at 500 rpm and add 80 gr of baked filtered Laponite powder gently during 20 seconds
- increase the speed to 1600 rpm for 30 minutes
- now, add 10 ml of NaCl solution
- continue for more 30 minutes at 1600 rpm
- and then turn off the mixer, leave the solution for eight days at rest for aging

As it is brought up before, viscosity of thixotropic yield stress fluids depends also on shear history of the sample, so what should we do to control the effect of shear history on result of rheometric tests? Figure 3.31 helps to comprehend better the issue.

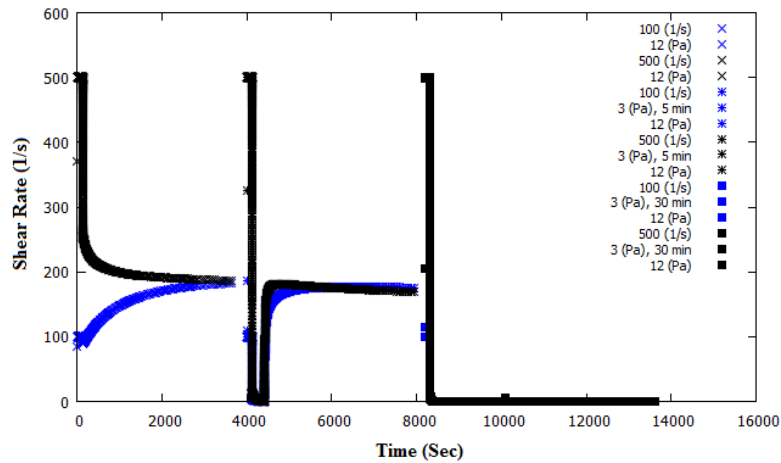


Figure 3.31: Shear history effect

Three batches of tests are introduced here, the main test is about to put the sample at constant shear stress of 12 Pa and measure the resultant shear rate, but the difference is; there are different pre-shear conditions for each test.

The results show that various shear history conditions hugely affect the viscosity and consequently the measured shear rate data. The same graph for each batch representing viscosity versus time is inserted here (See Figs. 3.32, 3.33, 3.34).

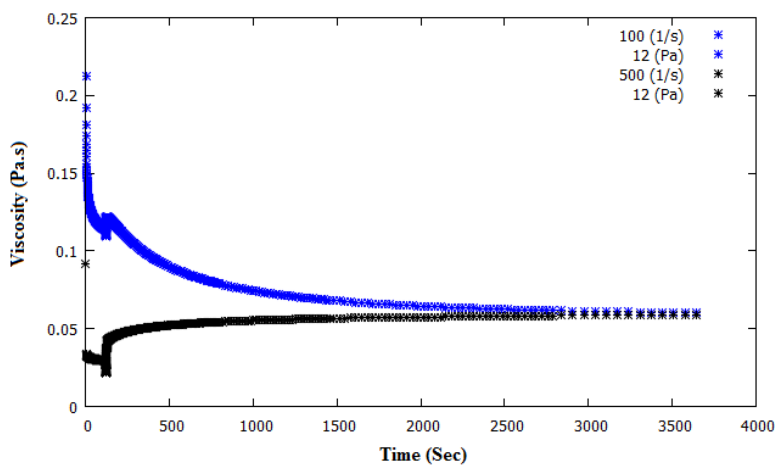


Figure 3.32: Structure destruction due to applied shear rates

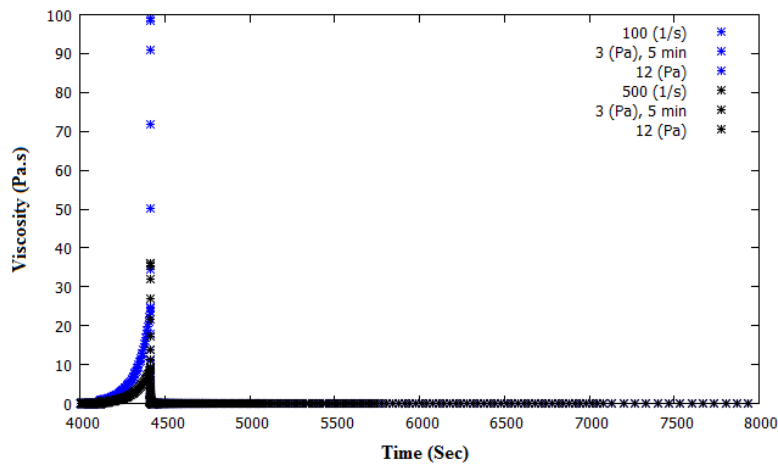


Figure 3.33: Structure build-up with applying a shear stress below the yield stress value - short duration

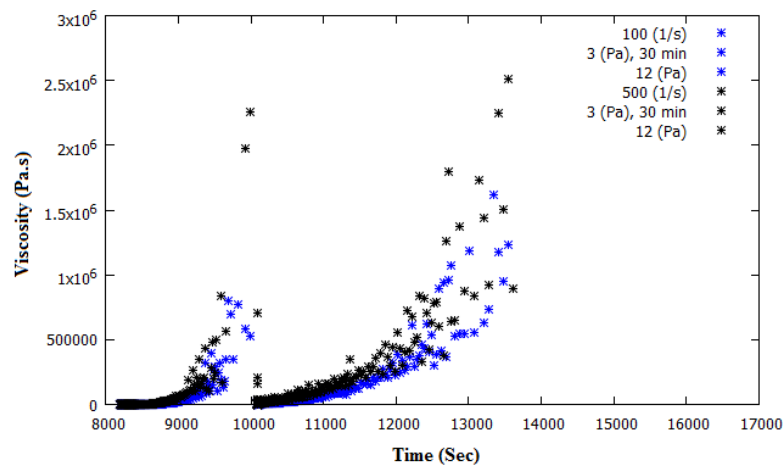


Figure 3.34: Structure build-up with applying a shear stress below the yield stress value - long duration

Figure (3.32) shows that with different levels of structure destruction before start of test, even after one hour already the viscosity and shear rate are not at the same steady state value.

However Figures (3.33 and 3.34) could be more helpful; at shear stress below the yield value, for shorter period, aging happens and viscosity increases but when the shear stress is exerted the structure breaks and flows. For longer period of build-up aging, viscosity increases dramatically and even after putting constant shear stress, the structure does not break and fluid becomes more and more viscous.

So the answer to what should we do to reduce the effect of shear history is embedded in these batches of tests. After loading the sample before every test starts, the fluid is put for 2 minutes at shear rate of 100 1/s which helps to make fluid uniform and then 10 minutes at rest to become structured, i.e. shear stress of 3 Pa which is assured to be beneath the yield value. Wholly this process provides

the same initial condition for each sample at every test. This kind of technique was used before by other authors [9, 94, 6, 41, 30].

Now let us start with characterization of thixotropic yield stress fluid (the Laponite suspension). The common flow curve test; shear stress versus shear rate, but at this case the test could be a little different because relatively long time is needed for Laponite suspension to reach steady state equilibrium. So, some chosen constant shear rate values were applied and after adequate time the steady shear stress were recorded and the flow curve was filled with these data points. It should be mentioned that for low shear rates the grooved recessed-end rotor and grooved cup geometry was used to guarantee no wall slip, and at high shear rates the DIN rotor and standard cup preferred to impede secondary flow issue. Figure (3.35) illustrates constant shear rate tests.

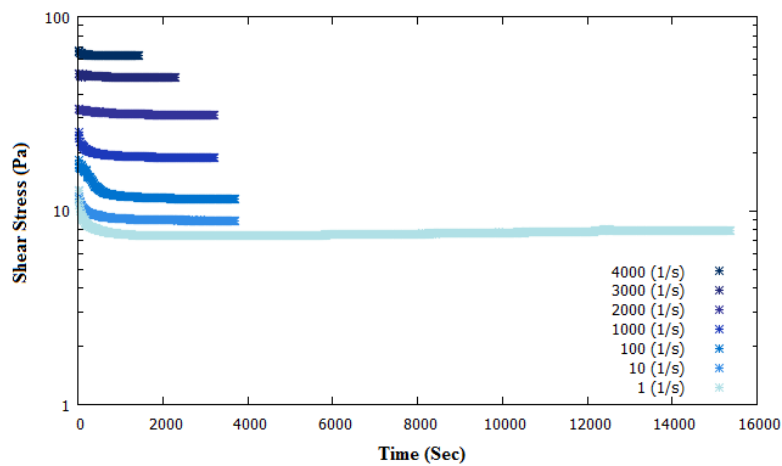


Figure 3.35: Laponite - constant shear rate, 4000-1 (1/s)

The resultant flow curve is presented here in figure (3.36).

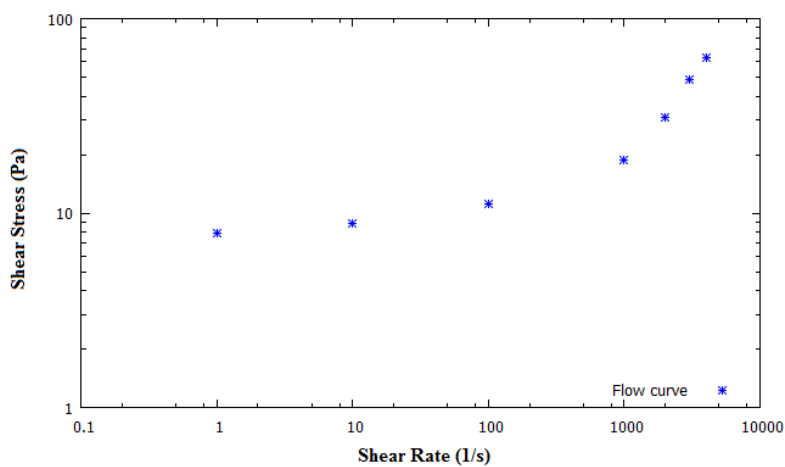


Figure 3.36: Laponite - flow curve, 4000-1 (1/s)

In continuance, to explore the fluid behavior at shear rates lower than 1 (1/s), even longer period of time is required till the fluid compartment becomes steady (See Fig. 3.37).

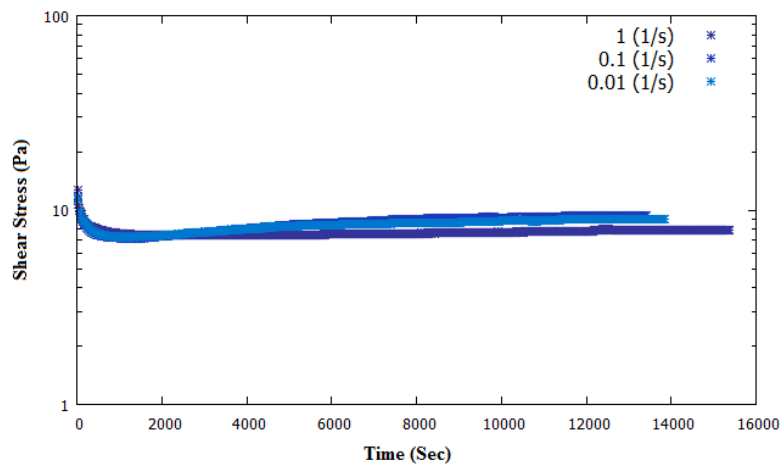


Figure 3.37: Laponite - constant shear rate, 1-0.01 (1/s)

An important element exposed in this figure is a struggle between shear rejuvenation and aging in all three tests.

And amended flow curve is given in figure (3.38).

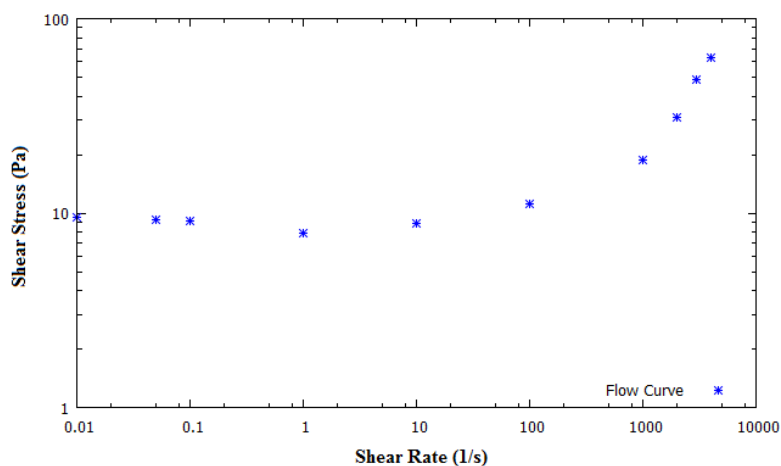


Figure 3.38: Laponite - flow curve

Regarding the flow curve, this is a non-monotonic one, what happening here is due to shear banding; a behavior exhibited by yield stress fluids. At sufficiently low shear rates the flow domain is divided into two parts: (a) the yielded region close to the shearing wall and (b) the unyielded region. In the unyielded region shear stress must essentially be lower than the yield value of the material while in the yielded region the shear stress should be higher than the yield stress [86, 58, 85, 42].

Each flow curve test of Laponite suspension took hours and it was being done in days using various suspensions. Thus to have a very reliable flow curve,

various test sets were performed to have a cloud of data and to make certain the repeatability.

The flow curve composed of three different data sets is inserted here in figure (3.39).

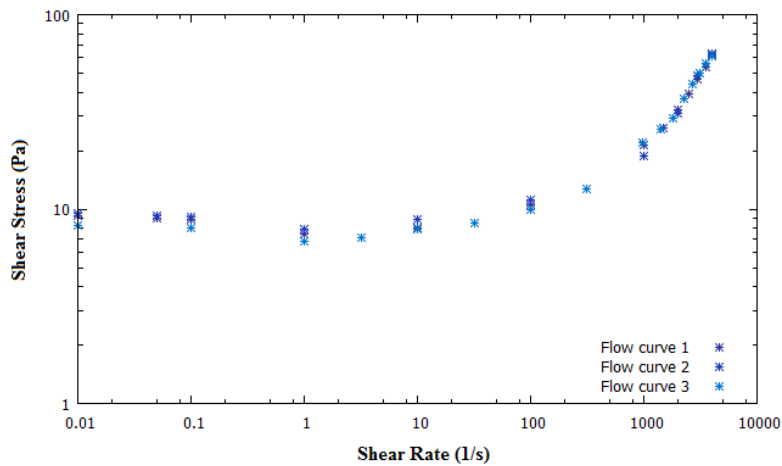


Figure 3.39: Laponite - flow curve, cloud of data points

Figure (3.40) asserts the data trend line is not in compliance to the Herschel-Bulkley fluid model which does not predict this abrupt transition.

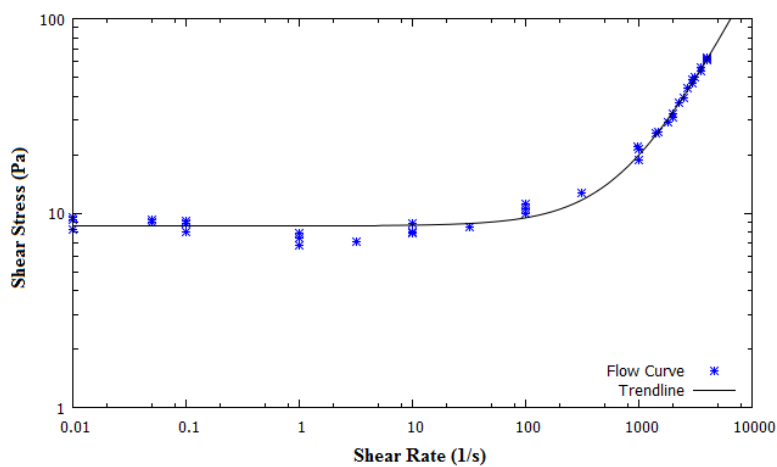


Figure 3.40: Laponite - flow curve, trend line

To measure a critical stress for Laponite solution, the creep tests with the same duration of 1 hour were run and results are illustrated in figure (3.41).

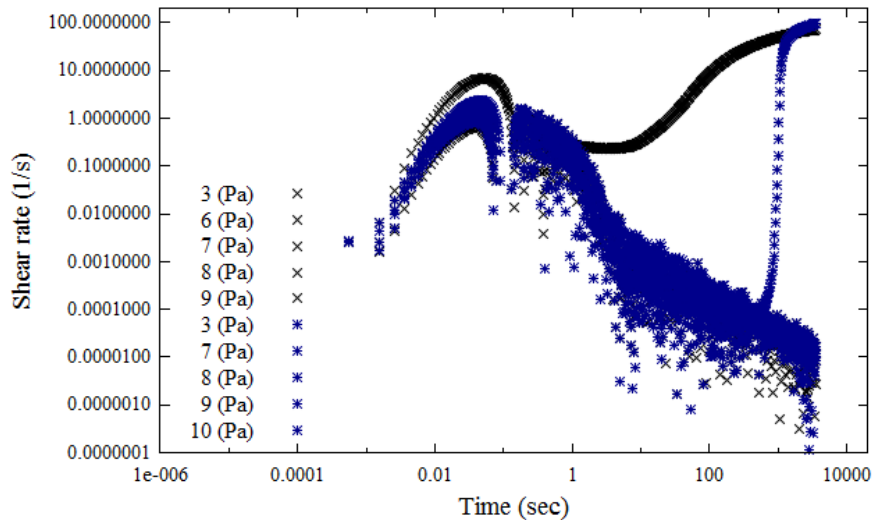


Figure 3.41: Laponite - creep tests

These data are responsible for two groups of tests using two different suspensions (shown in blue and black), critical stresses were measured as 9 and 10 pascal. It was not expected to have unique results but as the initial condition was set the same using aforesaid pre-shear process, the results are matched good enough.

Looking for a minimum pressure required to flow starts into the tube was carried out through the same directions held for hair gel. The minimum pressure was measured, converted to shear stress using Eq. (3.5.1) and then the results have been verified with rheometry.

It should be noted that for tests using the experimental setup, it was not possible to apply the same pre-shear process. At another side because bulk volume of sample is much larger, the effect of shear history is much less.

Before every test begins, the fluid put at rest until residual pressure reaches a stable minimum value and then test got started. Various tests were done to determine kind of statistical range as a result. In this case the non-Newtonian effective radius were used (See Fig. 3.42).

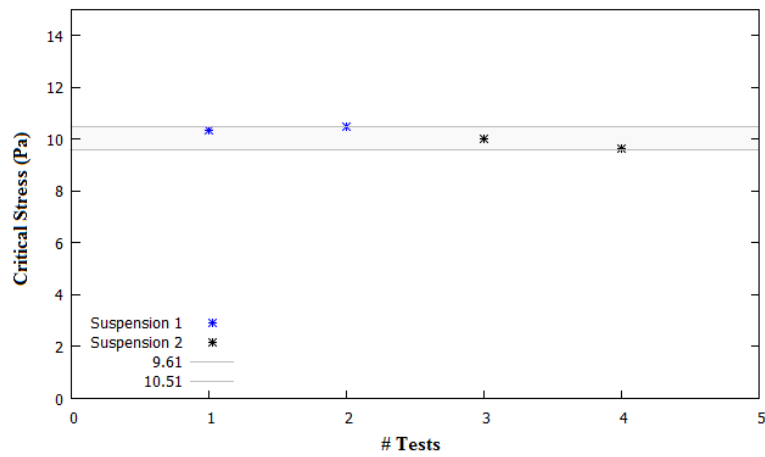


Figure 3.42: Laponite - critical stress, flow in tube

The range of critical stresses for rheometry and fluid in tube are in good agreement and again through combining rheometric and fluid transport investigations, the critical stress required for start up flow of thixotropic yield stress fluid was disclosed.

4

Final Discussion

As brought to your consideration, the minimum pressure or the critical stress which is necessary for startup flow of a simple yield stress fluid in tube was discovered, that value was validated using rheometric tests. The pressure-flow rate data of fluid in tube were measured and validated with Herschel-Bulckley solution which it means for any flow rate needed the required pressure value is known to apply. This is the firm first step toward study of gelled crude oils startup.

The second step was to explore the critical stress for a thixotropic yield stress fluid which by analogy would be a better representative for gelled crude oils. Also the obtained critical stress was double checked with rheometric experiments. The objective of this study is accomplished here which through combining fluid transport and rheometric tests, the pathway to find out the yield stress for this type of fluids was acknowledged and verified.

The comprehensive study needs a final step which could be as a future work, a proper non-Newtonian model is demanded to predict the behavior of thixotropic yield stress fluids which is a whole another extensive job. The proposed model is based on fluidity that is classically defined as the reciprocal of viscosity, parallel to this study, group of colleagues are working on this stuff. Numerous tests were performed to tune this model which as an example; transient structure break down-build up tests are inserted here in figure (4.1).

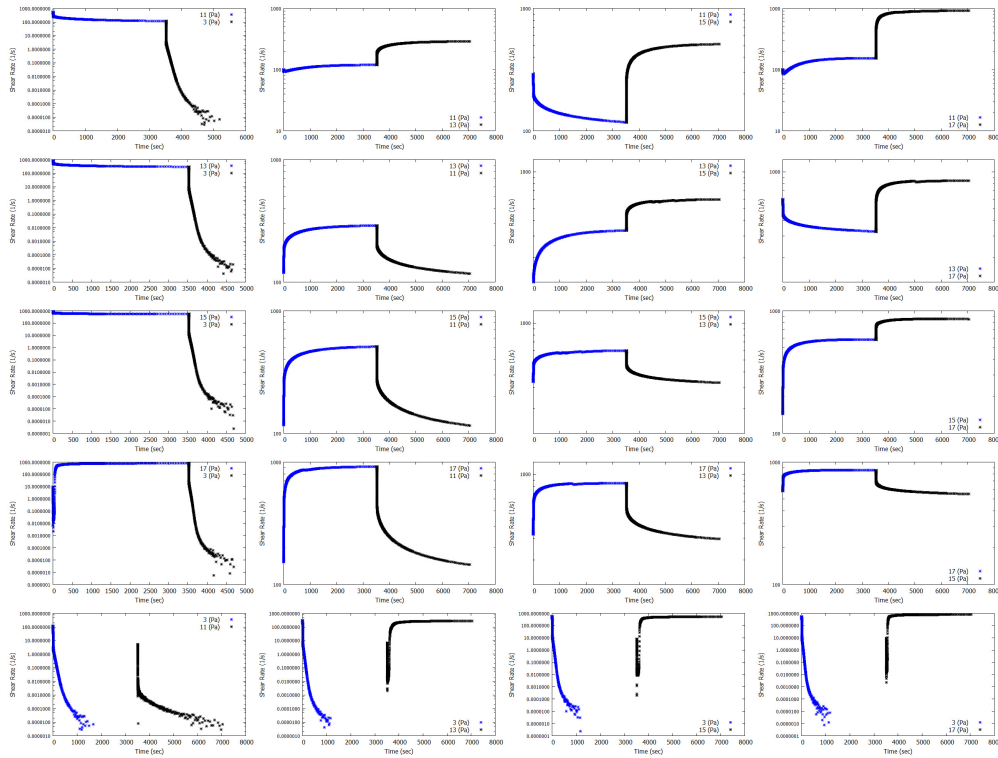


Figure 4.1: Transient structure build up - break down tests

When a robust model get ready, it would be tuned with gelled crude data and at that step likewise what done in this thesis, for any desired flow rate, the minimum pressure required is known. This could be the ultimate objective of whole these studies together.

Bibliography

- [1] B. ABOU, D. BONN, AND J. MEUNIER, *Nonlinear rheology of laponite suspensions under an external drive*, Journal of Rheology (1978-present), 47 (2003), pp. 979–988. 3.6
- [2] W. ALBRING, *Gk batchelor, an introduction to fluid dynamics. xviii+615 s. m. fig. cambridge 1967. university press. preis geb. 75 s. net*, ZAMM-Journal of Applied Mathematics and Mechanics/Zeitschrift für Angewandte Mathematik und Mechanik, 48 (1968), pp. 292–292. 2.2
- [3] B. K. ARAL AND D. M. KALYON, *Effects of temperature and surface roughness on time-dependent development of wall slip in steady torsional flow of concentrated suspensions*, Journal of Rheology (1978-present), 38 (1994), pp. 957–972. 2.2, 2.4
- [4] —, *Viscoelastic material functions of noncolloidal suspensions with spherical particles*, Journal of Rheology (1978-present), 41 (1997), pp. 599–620. 2.2
- [5] N. BALMFORTH AND R. CRASTER, *Geophysical aspects of non-newtonian fluid mechanics*, in Geomorphological fluid mechanics, Springer, 2001, pp. 34–51. 2.2
- [6] C. BARAVIAN, D. QUEMADA, AND A. PARKER, *A new methodology for rheological modeling of thixotropy applications to hydrocolloids*, in Proceedings of the XIIth International Congress on Rheology, Québec, Canada, 1996, pp. 779–780. 3.6.1
- [7] H. BARNES AND K. WALTERS, *The yield stress myth?*, Rheologica acta, 24 (1985), pp. 323–326. 2.1
- [8] H. A. BARNES, *A review of the slip (wall depletion) of polymer solutions, emulsions and particle suspensions in viscometers: its cause, character, and cure*, Journal of Non-Newtonian Fluid Mechanics, 56 (1995), pp. 221–251. 2.2, 2.4
- [9] —, *Thixotropy-a review*, Journal of Non-Newtonian fluid mechanics, 70 (1997), pp. 1–33. 2.1, 3.6.1
- [10] —, *The yield stress-a review or 'παντα ρει' -everything flows?*, Journal of Non-Newtonian Fluid Mechanics, 81 (1999), pp. 133–178. 1, 2.1

- [11] —, *The 'yield stress myth?' paper—21 years on*, Applied Rheology, 17 (2007), pp. 43110–44250. 2.1
- [12] J. BAUDRY, E. CHARLAIX, A. TONCK, AND D. MAZUYER, *Experimental evidence for a large slip effect at a nonwetting fluid-solid interface*, Langmuir, 17 (2001), pp. 5232–5236. 2.4
- [13] A. BERKER AND W. VAN ARSDALE, *Phenomenological models of viscoplastic, thixotropic, and granular materials*, Rheologica acta, 31 (1992), pp. 119–138. 2.2
- [14] V. BERTOLA, *A note on the effects of liquid viscoelasticity and wall slip on foam drainage*, Journal of Physics: Condensed Matter, 19 (2007), p. 246105. 2.2
- [15] R. B. BIRD, R. ARMSTRONG, AND O. HASSAGER, *Dynamics of polymeric liquids. vol. 1: Fluid mechanics*, (1987). 2.2
- [16] W. B. BLACK AND M. D. GRAHAM, *Wall-slip and polymer-melt flow instability*, Physical review letters, 77 (1996), p. 956. 2.2
- [17] E. BONACCURSO, H.-J. BUTT, AND V. S. CRAIG, *Surface roughness and hydrodynamic boundary slip of a newtonian fluid in a completely wetting system*, Physical review letters, 90 (2003), p. 144501. 2.4
- [18] D. BONN, H. KELLAY, H. TANAKA, G. WEGDAM, AND J. MEUNIER, *Laponite: What is the difference between a gel and a glass?*, Langmuir, 15 (1999), pp. 7534–7536. 3.6.1
- [19] D. BONN, S. TANASE, B. ABOU, H. TANAKA, AND J. MEUNIER, *Laponite: Aging and shear rejuvenation of a colloidal glass*, Physical review letters, 89 (2002), p. 015701. 3.6.1
- [20] P. E. BOUKANY AND S.-Q. WANG, *Exploring the transition from wall slip to bulk shearing banding in well-entangled dna solutions*, Soft Matter, 5 (2009), pp. 780–789. 2.4
- [21] R. BUSCALL, *Letter to the editor: Wall slip in dispersion rheometry*, Journal of Rheology (1978-present), 54 (2010), pp. 1177–1183. 2.4
- [22] C. CHANG, Q. D. NGUYEN, AND H. P. RØNNINGSEN, *Isothermal start-up of pipeline transporting waxy crude oil*, Journal of non-newtonian fluid mechanics, 87 (1999), pp. 127–154. 2

- [23] G.-S. CHANG, J.-S. KOO, K.-W. SONG, ET AL., *Wall slip of vaseline in steady shear rheometry*, Korea-Australia Rheology Journal, 15 (2003), pp. 55–61. 2.2, 2.4
- [24] C. CHEIKH AND G. KOPER, *Stick-slip transition at the nanometer scale*, Physical review letters, 91 (2003), p. 156102. 2.2
- [25] L. CHEN, Y. DUAN, C. ZHAO, AND L. YANG, *Rheological behavior and wall slip of concentrated coal water slurry in pipe flows*, Chemical Engineering and Processing: Process Intensification, 48 (2009), pp. 1241–1248. 2.2
- [26] Y. CHEN, D. KALYON, AND E. BAYRAMLI, *Wall slip behavior of linear low density polyethylene in capillary flow: Effect of materials of construction and surface roughness*, ANTEC 92–Shaping the Future., 1 (1992), pp. 1747–1751. 2.4
- [27] Y. CHEN, D. M. KALYON, AND E. BAYRAMLI, *Effects of surface roughness and the chemical structure of materials of construction on wall slip behavior of linear low density polyethylene in capillary flow*, Journal of applied polymer science, 50 (1993), pp. 1169–1177. 2.4
- [28] R. CHHABRA AND P. UHLHERR, *Static equilibrium and motion of spheres in viscoplastic liquids*, Encyclopedia of fluid mechanics, 7 (1988), pp. 611–633. 2.1
- [29] N. CHURAEV, V. SOBOLEV, AND A. SOMOV, *Slippage of liquids over lyophobic solid surfaces*, Journal of Colloid and Interface Science, 97 (1984), pp. 574–581. 2.2, 2.4
- [30] M. CLOITRE, R. BORREGA, AND L. LEIBLER, *Rheological aging and rejuvenation in microgel pastes*, Physical review letters, 85 (2000), p. 4819. 3.6.1
- [31] Y. COHEN AND A. METZNER, *Apparent slip flow of polymer solutions*, Journal of Rheology (1978-present), 29 (1985), pp. 67–102. 2.2, 2.4
- [32] B. COSTELLO, *The ar-g2 magnetic bearing rheometer*, TA Instruments Ltd, Fleming Way, Crawley, West Sussex RH10 9NB, (2005). 3.1.1
- [33] C. COTTIN-BIZONNE, B. CROSS, A. STEINBERGER, AND E. CHARLAIX, *Boundary slip on smooth hydrophobic surfaces: Intrinsic effects and possible artifacts*, Physical review letters, 94 (2005), p. 056102. 2.4
- [34] P. COUSSOT AND S. BOYER, *Determination of yield stress fluid behaviour from inclined plane test*, Rheologica acta, 34 (1995), pp. 534–543. 2.1

- [35] V. S. CRAIG, C. NETO, AND D. R. WILLIAMS, *Shear-dependent boundary slip in an aqueous newtonian liquid*, Physical review letters, 87 (2001), p. 054504. 2.2, 2.4
- [36] H. Z. CUMMINS, *Liquid, glass, gel: The phases of colloidal laponite*, Journal of Non-Crystalline Solids, 353 (2007), pp. 3891–3905. 3.6
- [37] M. A. DAY, *The no-slip condition of fluid dynamics*, Erkenntnis, 33 (1990), pp. 285–296. 2.2
- [38] D. DE KEE AND C. CHAN MAN FONG, *Rheological properties of structured fluids*, Polymer Engineering & Science, 34 (1994), pp. 438–445. 2.1
- [39] P. R. DE SOUZA MENDES, F. S.-M. DE ABREU SOARES, C. M. ZIGLIO, AND M. GONÇALVES, *Startup flow of gelled crudes in pipelines*, Journal of Non-Newtonian Fluid Mechanics, 179 (2012), pp. 23–31. 1
- [40] N. D. DENKOV, V. SUBRAMANIAN, D. GUROVICH, AND A. LIPS, *Wall slip and viscous dissipation in sheared foams: Effect of surface mobility*, Colloids and Surfaces A: Physicochemical and Engineering Aspects, 263 (2005), pp. 129–145. 2.4
- [41] C. DEREK, A. AJDARI, G. DUCOURET, AND F. LEQUEUX, *Rheological characterization of aging in a concentrated colloidal suspension*, Comptes Rendus de l'Académie des Sciences-Series IV-Physics, 1 (2000), pp. 1115–1119. 3.6.1
- [42] T. DIVOUX, D. TAMARII, C. BARENTIN, AND S. MANNEVILLE, *Transient shear banding in a simple yield stress fluid*, Physical review letters, 104 (2010), p. 208301. 2.4, 3.6.1
- [43] N. DOE, *Rheometer torque calibration fixture*, May 5 2009. US Patent 7,526,941. 3.1.2, 3.1.2, 3.1.2, 3.1.2, 3.1.2
- [44] N. DOE AND P. FOSTER, *System and method for automatic identification of a detachable component of an instrument*, Oct. 11 2005. US Patent 6,952,950. 3.1.2, 3.1.2, 3.1.2, 3.1.2, 3.1.2
- [45] R. DURAIRAJ, S. MALLIK, A. SEMAN, AND N. EKERE, *Investigation of wall-slip effect on lead-free solder paste and isotropic conductive adhesives*, Sadhana, 34 (2009), pp. 799–810. 2.4
- [46] N. Q. DZUY AND D. V. BOGER, *Yield stress measurement for concentrated suspensions*, Journal of Rheology (1978-present), 27 (1983), pp. 321–349. 2.1

- [47] H. EGGER AND K. M. MCGRATH, *Estimating depletion layer thickness in colloidal systems: Correlation with oil-in-water emulsion composition*, Colloids and Surfaces A: Physicochemical and Engineering Aspects, 275 (2006), pp. 107–113. 2.2, 2.4
- [48] M. ESCUDIER AND F. PRESTI, *Pipe flow of a thixotropic liquid*, Journal of non-newtonian fluid mechanics, 62 (1996), pp. 291–306. 3.6
- [49] I. D. EVANS, *Letter to the editor: on the nature of the yield stress*, Journal of Rheology (1978-present), 36 (1992), pp. 1313–1318. 2.1
- [50] J. FRANCO, C. GALLEGOS, AND H. BARNES, *On slip effects in steady-state flow measurements of oil-in-water food emulsions*, Journal of Food Engineering, 36 (1998), pp. 89–102. 2.2, 2.4
- [51] T. S. GOLCZYNSKI AND E. C. KEMPTON, *Understanding wax problems leads to deepwater flow assurance solutions*, World oil, 227 (2006). 1
- [52] J. GOSHAWK, D. BINDING, D. KELL, AND R. GOODACRE, *Rheological phenomena occurring during the shearing flow of mayonnaise*, Journal of Rheology (1978-present), 42 (1998), pp. 1537–1553. 2.2
- [53] R. GOVARDHAN, G. SRINIVAS, A. ASTHANA, AND M. BOBJI, *Time dependence of effective slip on textured hydrophobic surfaces*, Physics of Fluids (1994-present), 21 (2009), p. 052001. 2.4
- [54] J. P. HARTNETT AND R. Y. HU, *Technical note: the yield stress-an engineering reality*, Journal of Rheology (1978-present), 33 (1989), pp. 671–679. 2.1
- [55] S. HATZIKIRIAKOS AND J. DEALY, *Wall slip of molten high density polyethylene. i. sliding plate rheometer studies*, Journal of Rheology (1978-present), 35 (1991), pp. 497–523. 2.4
- [56] H. HERVET AND L. LÉGER, *Flow with slip at the wall: from simple to complex fluids*, Comptes rendus physique, 4 (2003), pp. 241–249. 2.2
- [57] F. HOLLAND AND R. BRAGG, *Fluid Flow for Chemical and Process Engineers*, Butterworth-Heinemann, 1995. 2.2
- [58] N. HUANG, G. OVARLEZ, F. BERTRAND, S. RODTS, P. COUSSOT, AND D. BONN, *Flow of wet granular materials*, Physical review letters, 94 (2005), p. 028301. 3.6.1

- [59] A. JAMES, D. WILLIAMS, AND P. WILLIAMS, *Direct measurement of static yield properties of cohesive suspensions*, *Rheologica Acta*, 26 (1987), pp. 437–446. 2.1, 2.3
- [60] P. JOSEPH AND P. TABELING, *Direct measurement of the apparent slip length*, *Physical Review E*, 71 (2005), p. 035303. 2.4
- [61] Y. M. JOSHI, A. K. LELE, AND R. MASHELKAR, *Slipping fluids: a unified transient network model*, *Journal of non-newtonian fluid mechanics*, 89 (2000), pp. 303–335. 2.2
- [62] D. M. KALYON, *Apparent slip and viscoplasticity of concentrated suspensions*, *Journal of Rheology (1978-present)*, 49 (2005), pp. 621–640. 2.2
- [63] D. M. KALYON, P. YARAS, B. ARAL, AND U. YILMAZER, *Rheological behavior of a concentrated suspension: A solid rocket fuel simulant*, *Journal of Rheology (1978-present)*, 37 (1993), pp. 35–53. 2.2, 2.3, 2.4
- [64] T. KILJAŃSKI, *A method for correction of the wall-slip effect in a couette rheometer*, *Rheologica acta*, 28 (1989), pp. 61–64. 2.2
- [65] M. KROON, W. L. VOS, AND G. H. WEGDAM, *Structure and formation of a gel of colloidal disks*, *Physical Review E*, 57 (1998), p. 1962. 3.6
- [66] N. R. KUMAR, K. MURALIDHAR, AND Y. M. JOSHI, *On the refractive index of ageing dispersions of laponite*, *Applied Clay Science*, 42 (2008), pp. 326–330. 3.6.1
- [67] P. KUNDU AND I. COHEN, *Fluid mechanics, 4th edn*, 2008. 2.2
- [68] J. LABANDA AND J. LLORENS, *Rheology of laponite colloidal dispersions modified by sodium polyacrylates*, *Colloids and Surfaces A: Physicochemical and Engineering Aspects*, 249 (2004), pp. 127–129. 3.6.1
- [69] J. LABANDA AND J. LLORENS, *Influence of sodium polyacrylate on the rheology of aqueous laponite dispersions*, *Journal of colloid and interface science*, 289 (2005), pp. 86–93. 3.6, 3.6.1
- [70] Y. LAM, Z. WANG, X. CHEN, AND S. JOSHI, *Wall slip of concentrated suspension melts in capillary flows*, *Powder Technology*, 177 (2007), pp. 162–169. 2.2
- [71] R. G. LARSON, *The structure and rheology of complex fluids*, vol. 33, Oxford university press New York, 1999. 2.2, 2.4

- [72] A. LAWAL AND D. M. KALYON, *Squeezing flow of viscoplastic fluids subject to wall slip*, Polymer Engineering & Science, 38 (1998), pp. 1793–1804. 2.2, 2.4
- [73] H. S. LEE, P. SINGH, W. H. THOMASON, AND H. S. FOGLER, *Waxy oil gel breaking mechanisms: adhesive versus cohesive failure*, Energy & Fuels, 22 (2007), pp. 480–487. 2.2
- [74] A. LINDNER, P. COUSSOT, AND D. BONN, *Viscous fingering in a yield stress fluid*, Physical Review Letters, 85 (2000), p. 314. 2.3, 2.4
- [75] S. LUK, R. MUTHARASAN, AND D. APELIAN, *Experimental observations of wall slip: tube and packed bed flow*, Industrial & engineering chemistry research, 26 (1987), pp. 1609–1616. 2.2, 2.4
- [76] A. MACIEL, V. SALAS, J. SOLTERO, J. GUZMÁN, AND O. MANERO, *On the wall slip of polymer blends*, Journal of Polymer Science Part B: Polymer Physics, 40 (2002), pp. 303–316. 2.2
- [77] C. W. MACOSKO AND R. G. LARSON, *Rheology: principles, measurements, and applications*, (1994). 2.1
- [78] A. MAGNIN AND J. PIAU, *Cone-and-plate rheometry of yield stress fluids. study of an aqueous gel*, Journal of Non-Newtonian Fluid Mechanics, 36 (1990), pp. 85–108. 2.3, 2.4
- [79] S. P. MEEKER, R. T. BONNECAZE, AND M. CLOITRE, *Slip and flow in soft particle pastes*, Physical review letters, 92 (2004), p. 198302. 2.2, 2.3
- [80] G. H. MEETEN, *Squeeze flow of soft solids between rough surfaces*, Rheologica acta, 43 (2004), pp. 6–16. 2.2, 2.4
- [81] J. MEWIS, *Thixotropy-a general review*, Journal of Non-Newtonian Fluid Mechanics, 6 (1979), pp. 1–20. 2.1
- [82] K. MIGLER, H. HERVET, AND L. LEGER, *Slip transition of a polymer melt under shear stress*, Physical review letters, 70 (1993), p. 287. 2.2
- [83] P. MØLLER, A. FALL, AND D. BONN, *Origin of apparent viscosity in yield stress fluids below yielding*, EPL (Europhysics Letters), 87 (2009), p. 38004. 2.2
- [84] P. MOLLER, A. FALL, V. CHIKKADI, D. DERKS, AND D. BONN, *An attempt to categorize yield stress fluid behaviour*, Philosophical Transactions

- of the Royal Society of London A: Mathematical, Physical and Engineering Sciences, 367 (2009), pp. 5139–5155. 2.1
- [85] P. MØLLER, S. RODTS, M. MICHELS, AND D. BONN, *Shear banding and yield stress in soft glassy materials*, Physical Review E, 77 (2008), p. 041507. 3.6.1
- [86] P. C. MØLLER, J. MEWIS, AND D. BONN, *Yield stress and thixotropy: on the difficulty of measuring yield stresses in practice*, Soft matter, 2 (2006), pp. 274–283. 3.6.1
- [87] P. MONGONDRY, J. F. TASSIN, AND T. NICOLAI, *Revised state diagram of laponite dispersions*, Journal of colloid and interface science, 283 (2005), pp. 397–405. 3.6
- [88] M. MOONEY, *Explicit formulas for slip and fluidity*, Journal of Rheology (1929-1932), 2 (1931), pp. 210–222. 2.2
- [89] A. MOURCHID, A. DELVILLE, J. LAMBARD, E. LECOLIER, AND P. LEVITZ, *Phase diagram of colloidal dispersions of anisotropic charged particles: equilibrium properties, structure, and rheology of laponite suspensions*, Langmuir, 11 (1995), pp. 1942–1950. 3.6
- [90] A. MOURCHID, E. LECOLIER, H. VAN DAMME, AND P. LEVITZ, *On viscoelastic, birefringent, and swelling properties of laponite clay suspensions: revisited phase diagram*, Langmuir, 14 (1998), pp. 4718–4723. 3.6, 3.6
- [91] A. MUJUMDAR, A. N. BERIS, AND A. B. METZNER, *Transient phenomena in thixotropic systems*, Journal of Non-Newtonian Fluid Mechanics, 102 (2002), pp. 157–178. 2.1
- [92] C. NETO, V. CRAIG, AND D. WILLIAMS, *Evidence of shear-dependent boundary slip in newtonian liquids*, The European Physical Journal E, 12 (2003), pp. 71–74. 2.2
- [93] C. NETO, D. R. EVANS, E. BONACCURSO, H.-J. BUTT, AND V. S. CRAIG, *Boundary slip in newtonian liquids: a review of experimental studies*, Reports on Progress in Physics, 68 (2005), p. 2859. 2.2, 2.4
- [94] Q. NGUYEN AND D. BOGER, *Thixotropic behaviour of concentrated bauxite residue suspensions*, Rheologica Acta, 24 (1985), pp. 427–437. 3.6.1
- [95] —, *Measuring the flow properties of yield stress fluids*, Annual Review of Fluid Mechanics, 24 (1992), pp. 47–88. 2.1, 2.2, 2.3, 2.4

- [96] H. OERTEL, P. ERHARD, K. ASFAW, D. ETLING, U. MULLER, U. RIEDEL, K. SREENIVASAN, AND J. WARNATZ, *Prandtl-essentials of fluid mechanics*, vol. 158, Springer Science & Business Media, 2010. 2.2
- [97] R. PAL, *Slippage during the flow of emulsions in rheometers*, Colloids and Surfaces A: Physicochemical and Engineering Aspects, 162 (2000), pp. 55–66. 2.2, 2.4
- [98] N. PASHIAS, D. BOGER, J. SUMMERS, AND D. GLENISTER, *A fifty cent rheometer for yield stress measurement*, Journal of Rheology (1978-present), 40 (1996), pp. 1179–1189. 2.1
- [99] J. PERSELLO, A. MAGNIN, J. CHANG, J. PIAU, AND B. CABANE, *Flow of colloidal aqueous silica dispersions*, Journal of Rheology (1978-present), 38 (1994), pp. 1845–1870. 2.4
- [100] T. PETERFI, *Arch. entwicklungsmech.*, Organ, 112 (1927), p. 680. 2.1
- [101] R. PIT, H. HERVET, AND L. LÉGER, *Friction and slip of a simple liquid at a solid surface*, Tribology letters, 7 (1999), pp. 147–152. 2.2
- [102] R. PIT, H. HERVET, AND L. LEGER, *Direct experimental evidence of slip in hexadecane: solid interfaces*, Physical review letters, 85 (2000), p. 980. 2.2, 2.4
- [103] D. J. PLAZEK, *Magnetic bearing torsional creep apparatus*, Journal of Polymer Science Part A-2: Polymer Physics, 6 (1968), pp. 621–638. 3.1.1
- [104] J. PLUCINSKI, R. K. GUPTA, AND S. CHAKRABARTI, *Wall slip of mayonnaises in viscometers*, Rheologica acta, 37 (1998), pp. 256–269. 2.2, 2.3, 2.4
- [105] H. PRINCEN, *Rheology of foams and highly concentrated emulsions. ii. experimental study of the yield stress and wall effects for concentrated oil-in-water emulsions*, Journal of colloid and interface science, 105 (1985), pp. 150–171. 2.3, 2.4
- [106] J. PRYCE-JONES, *17 (1934) 305; 19 (1936) 395*, JOCCA, 26 (1943), p. 3. 2.1
- [107] J. RATULOWSKI, A. AMIN, A. HAMMAMI, M. MUHAMMAD, M. RIDING, ET AL., *Flow assurance and subsea productivity: closing the loop with connectivity and measurements*, in SPE Annual Technical Conference and Exhibition, Society of Petroleum Engineers, 2004. 1

- [108] M. RUIZ-VIERA, M. DELGADO, J. FRANCO, AND C. GALLEGOS, *Evaluation of wall slip effects in the lubricating grease/air two-phase flow along pipelines*, Journal of Non-Newtonian Fluid Mechanics, 139 (2006), pp. 190–196. 2.2, 2.3, 2.4
- [109] W. B. RUSSEL AND M. C. GRANT, *Distinguishing between dynamic yielding and wall slip in a weakly flocculated colloidal dispersion*, Colloids and Surfaces A: Physicochemical and Engineering Aspects, 161 (2000), pp. 271–282. 2.2, 2.3
- [110] B. RUZICKA, L. ZULIAN, AND G. RUOCCO, *More on the phase diagram of laponite*, Langmuir, 22 (2006), pp. 1106–1111. 3.6
- [111] S. SAINTPERE, B. HERZHAFT, A. TOURE, S. JOLLET, ET AL., *Rheological properties of aqueous foams for underbalanced drilling*, in SPE Annual Technical Conference and Exhibition, Society of Petroleum Engineers, 1999. 2.3, 2.4
- [112] M. SÁNCHEZ, C. VALENCIA, J. FRANCO, AND C. GALLEGOS, *Wall slip phenomena in oil-in-water emulsions: effect of some structural parameters*, Journal of colloid and interface science, 241 (2001), pp. 226–232. 2.2
- [113] E. SCHNELL, *Slippage of water over nonwetttable surfaces*, Journal of Applied Physics, 27 (1956), pp. 1149–1152. 2.4
- [114] J. SCHURZ, *The yield stress-an empirical reality*, Rheologica acta, 29 (1990), pp. 170–171. 2.1
- [115] J. R. SETH, M. CLOITRE, AND R. T. BONNECAZE, *Influence of short-range forces on wall-slip in microgel pastes*, Journal of Rheology (1978-present), 52 (2008), pp. 1241–1268. 2.2, 2.3, 2.4
- [116] T. SOCHI, *Slip at fluid-solid interface*, Polymer Reviews, 51 (2011), pp. 309–340. 2.2
- [117] K. SORBIE, *Depleted layer effects in polymer flow through porous media: I. single capillary calculations*, Journal of colloid and interface science, 139 (1990), pp. 299–314. 2.2
- [118] R. D. SPAANS AND M. C. WILLIAMS, *Letter to the editor: At last, a true liquid-phase yield stress*, Journal of Rheology (1978-present), 39 (1995), pp. 241–246. 2.1

- [119] G. SPATHIS AND C. MAGGANA, *A non-linear viscoelastic model for predicting the yield stress of amorphous polymers*, *Polymer*, 38 (1997), pp. 2371–2377. 2.2, 2.3
- [120] S. P. SUTERA AND R. SKALAK, *The history of poiseuille’s law*, *Annual Review of Fluid Mechanics*, 25 (1993), pp. 1–20. 3.3
- [121] H. TANAKA, J. MEUNIER, AND D. BONN, *Nonergodic states of charged colloidal suspensions: repulsive and attractive glasses and gels*, *Physical Review E*, 69 (2004), p. 031404. 3.6, 3.6
- [122] D. W. THOMPSON AND J. T. BUTTERWORTH, *The nature of laponite and its aqueous dispersions*, *Journal of Colloid and Interface Science*, 151 (1992), pp. 236–243. 3.6
- [123] C. TROPEA, A. L. YARIN, AND J. F. FOSS, *Springer handbook of experimental fluid mechanics*, vol. 1, Springer Science & Business Media, 2007. 2.4
- [124] P. UHLHERR, K. PARK, C. TIU, AND J. ANDREWS, *Yield stress from fluid behaviour on an inclined plane*, *Advances in Rheology*, 2 (1984), pp. 183–190. 2.1
- [125] S. VAN KAO, L. E. NIELSEN, AND C. T. HILL, *Rheology of concentrated suspensions of spheres. i. effect of the liquid-solid interface*, *Journal of Colloid and Interface Science*, 53 (1975), pp. 358–366. 2.4
- [126] V. VAND, *Viscosity of solutions and suspensions. i. theory*, *The Journal of Physical Chemistry*, 52 (1948), pp. 277–299. 2.2
- [127] R. VENKATESAN, N. NAGARAJAN, K. PASO, Y.-B. YI, A. SASTRY, AND H. FOGLER, *The strength of paraffin gels formed under static and flow conditions*, *Chemical Engineering Science*, 60 (2005), pp. 3587–3598. 2
- [128] R. VENKATESAN, J.-A. ÖSTLUND, H. CHAWLA, P. WATTANA, M. NYDÉN, AND H. S. FOGLER, *The effect of asphaltenes on the gelation of waxy oils*, *Energy & fuels*, 17 (2003), pp. 1630–1640. 2
- [129] R. F. VISINTIN, R. LAPASIN, E. VIGNATI, P. D’ANTONA, AND T. P. LOCKHART, *Rheological behavior and structural interpretation of waxy crude oil gels*, *Langmuir*, 21 (2005), pp. 6240–6249. 2
- [130] R. F. VISINTIN, T. P. LOCKHART, R. LAPASIN, AND P. D’ANTONA, *Structure of waxy crude oil emulsion gels*, *Journal of Non-Newtonian Fluid Mechanics*, 149 (2008), pp. 34–39. 2

- [131] H. WALLS, S. B. CAINES, A. M. SANCHEZ, AND S. A. KHAN, *Yield stress and wall slip phenomena in colloidal silica gels*, *Journal of Rheology* (1978-present), 47 (2003), pp. 847–868. 2.2, 2.3, 2.4
- [132] L. WARDHAUGH AND D. BOGER, *Flow characteristics of waxy crude oils: application to pipeline design*, *AIChE Journal*, 37 (1991), pp. 871–885. 2
- [133] R. WESTOVER, *The significance of slip of polymer melt flow*, *Polymer Engineering & Science*, 6 (1966), pp. 83–89. 2.3
- [134] C. YAN-YAN, Y. HOU-HUI, AND L. HUA-BING, *Boundary slip and surface interaction: a lattice boltzmann simulation*, *Chinese Physics Letters*, 25 (2008), p. 184. 2.2
- [135] Y. L. YEOW, B. CHOON, L. KARNIAWAN, AND L. SANTOSO, *Obtaining the shear rate function and the slip velocity function from couette viscometry data*, *Journal of non-newtonian fluid mechanics*, 124 (2004), pp. 43–49. 2.2